HHS Public Access

Author manuscript

Cell Rep. Author manuscript; available in PMC 2020 May 05.

Published in final edited form as:

Cell Rep. 2020 March 24; 30(12): 4065–4081.e4. doi:10.1016/j.celrep.2020.03.002.

IQGAP1 Negatively Regulates HIV-1 Gag Trafficking and Virion Production

Yosef Sabo[1,2,3,4], **Kenia de los Santos**[1,2,3], **Stephen P. Goff**[1,2,3,5,*]

[1]Howard Hughes Medical Institute, Columbia University, New York, NY 10032, USA

[2]Department of Biochemistry and Molecular Biophysics, Columbia University, New York, NY 10032, USA

[3]Department of Microbiology and Immunology, Columbia University, New York, NY 10032, USA

[4]Department of Medicine, Division of Infectious Diseases, Columbia University, New York, NY 10032, USA

[5]Lead Contact

SUMMARY

IQGAP1 is a master regulator of many cellular processes, including intracellular vesicle trafficking and endocytosis. We show that depletion of IQGAP1 in a variety of cell types increases the release of HIV-1 infectious virions and that overexpression diminishes virion production, with neither affecting the early stages of infection. IQGAP1 negatively regulates the steady-state levels of HIV-1 Gag at the plasma membrane, the site of assembly. We establish that IQGAP1 interacts with both the nucleocapsid and p6 domains of Gag, and interaction with either domain is sufficient for its regulatory function. Finally, we demonstrate that IQGAP1 regulation is independent of HIV-1 Gag “late-domains” sequences required by the virus to recruit the cellular ESCRT machinery. Thus, we provide evidence that IQGAP1 is a negative regulatory factor inhibiting efficient budding of HIV-1 by reducing Gag accumulation at the plasma membrane.

Graphical Abstract

*Correspondence: spg1@cumc.columbia.edu.

AUTHOR CONTRIBUTIONS

Y.S. and S.P.G. designed the experiments. Y.S. and S.P.G. wrote the manuscript. Y.S. and K.d.l.S. performed the experiments.

SUPPLEMENTAL INFORMATION

Supplemental Information can be found online at https://doi.org/10.1016/j.celrep.2020.03.002.

DECLARATION OF INTERESTS

The authors declare no competing interests.

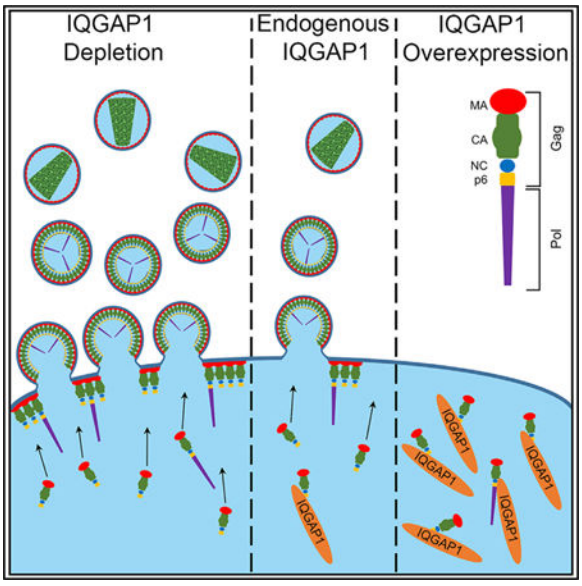

In Brief

IQGAP1 is a ubiquitously expressed master regulator of many cellular processes, including intracellular trafficking. Sabo et al. demonstrate that in a variety of cell types, IQGAP1 acts as a negative regulator of HIV-1 viral particle release by reducing accumulation of the Gag viral structural protein at the plasma membrane.

INTRODUCTION

The assembly and release of human immunodeficiency virus type 1 (HIV-1) virion particles from infected cells is orchestrated by the viral Gag and Gag-Pol precursor proteins $Pr55^{gag}$ and $Pr160^{gag\text{-}pol}$ but involves both viral and cellular proteins. The Gag and Gag-Pol proteins are translated in the cytoplasm and are co-translationally modified by the addition of N-terminal myristate (Göttlinger et al., 1989; Pal et al., 1990), which is required for their targeting to the host plasma membrane (Bouamr et al., 2003; Bryant and Ratner, 1990; Ono and Freed, 1999; Saad et al., 2007; Zhou and Resh, 1996). At the plasma membrane the $Pr55^{gag}$ and $Pr160^{gag\text{-}pol}$ proteins multimerize and form a spherical bud structure bulged toward the exterior of the cell. To reach the plasma membrane, the cytoplasmic Gag and Gag-Pol proteins must travel along the cellular cytoskeleton and transverse the dense and dynamic network of filamentous actin that resides beneath it (Fackler and Kräusslich, 2006; Naghavi and Goff, 2007). During their transit to the plasma membrane, the HIV-1 Gag proteins “hijack” components of the ESCRT host factors using two different late-domain motifs, the PTAP and the $LYP(X)_nL$ sequences, that are present in their C termini (Sundquist and Kräusslich, 2012). The ESCRT machinery, which is composed of many protein complexes (Henne et al., 2011; Schmidt and Teis, 2012), participates in a variety of cellular processes that all have in common the scission of membrane necks from the inside (Christ et al., 2017; Hurley and Hanson, 2010). Many enveloped viruses, including HIV-1, take advantage of the ESCRT pathway by interacting with specific proteins from this machinery to complete their late stages of virion production (Votteler and Sundquist, 2013). For HIV-1,

the PTAP late-domain sequence mediates an interaction with the TSG101 protein (Garrus et al., 2001; Martin-Serrano et al., 2001; VerPlank et al., 2001), while the $LYP(X)_nL$ sequence mediates interaction with the Alix protein (Strack et al., 2003), both key proteins of the ESCRT pathway (Henne et al., 2011; Schmidt and Teis, 2012). The assembly process ends when the neck of the bud is fissioned using the hijacked ESCRT machinery and the enveloped viral particle is then released from the host cell (Sundquist and Kräusslich, 2012). Following release from the host cell, the viral particles undergo a maturation step that is driven by the viral protease and results in the cleavage of the $Pr55^{gag}$ and $Pr160^{gag\text{-}pol}$ proteins to form the fully processed virion proteins (Sundquist and Kräusslich, 2012).

The IQGAP proteins are major cytoskeleton regulators that affect both microtubules and actin (Abel et al., 2015; Briggs and Sacks, 2003; Mateer et al., 2003; Noritake et al., 2005; Watanabe et al., 2015; White et al., 2012). IQGAPs, found in all eukaryotes, are a family of large, evolutionarily highly conserved scaffold proteins. They bind and regulate the functions of a vast array of interacting proteins that take part in many cellular processes, including cell migration and adherence, cytokinesis, intracellular vesicle trafficking, endo- and exocytosis, cell signaling, and regulation of numerous nuclear functions (reviewed in Abel et al., 2015; Choi and Anderson, 2016; Hedman et al., 2015; Noordstra and Akhmanova, 2017; Smith et al., 2015; Watanabe et al., 2015). Mammals express three isoforms of IQGAPs, termed IQGAP1, IQGAP2, and IQGAP3. All share similar structures and domains that mediate protein-protein interactions, but they display distinct tissue-specific patterns of expression (Abel et al., 2015; Briggs and Sacks, 2003; Hedman et al., 2015; Mateer et al., 2003; Noritake et al., 2005; White et al., 2012). IQGAP1, the best-characterized IQGAP isoform, is expressed ubiquitously.

The involvement of IQGAP1 in the regulation of various cellular pathways, many of which involve the cellular cytoskeleton, makes this protein an important host factor for many pathogens. Indeed, IQGAP1 has been documented as a positive factor for the replication of several viruses, often playing an essential role in the late stages of their life cycle. Our lab previously reported that IQGAP1 is important for spreading infections of the Moloney murine leukemia virus (MMuLV) (Leung et al., 2006). The MA domain in the MMuLV Gag protein interacts with IQGAP1, and mutations that disrupt this interaction or depletion of IQGAP1 hindered the ability of the virus to spread in culture (Leung et al., 2006). IQGAP1 has been also demonstrated as an essential host factor for the budding of enveloped viruses from the *Filoviridae* and *Flaviviridae* families. IQGAP1 interacts with the VP40 Matrix protein of the Ebola virus and is required for the budding of VP40 virus-like particles (VLPs) (Lu et al., 2013). IQGAP1 is localized within cellular inclusion bodies induced by the Marburg virus and enhances viral release (Dolnik et al., 2014). IQGAP1 also interacts with the classical swine fever virus core protein, and this interaction was found to be important for efficient viral egress (Gladue et al., 2011). Last, IQGAP1 was detected in purified HIV-1 viral particles (Chertova et al., 2006), though the significance of its packaging or its role in HIV-1 assembly remains unknown.

Here we report that IQGAP1 restricts the efficient release of HIV-1 progeny virions. We find that knockdown (KD) or knockout (KO) of IQGAP1 increases HIV-1 infectious virion production, while overexpression of IQGAP1 dramatically decreases HIV-1 particle release.

Furthermore, we show that IQGAP1 interacts with two domains within the HIV-1 Gag protein, the nucleocapsid (NC) and p6 domains, and that interaction with either is sufficient for its activity. Finally, we demonstrate that IQGAP1 negatively regulates the membrane association of HIV-1 Gag and that this regulation is independent of the ability of Gag to recruit and use the cellular ESCRT machinery. We propose that for HIV-1, IQGAP1 acts as a negative cellular factor preventing the accumulation of viral Gag proteins at the cellular plasma membrane by interacting with their C-terminal region, thereby hindering their function to drive viral budding.

RESULTS

Depletion of IQGAP1 Increases Production of Infectious HIV-1 Virions

To test for the potential involvement of IQGAP1 in the late stage of HIV-1 life cycle, control and IQGAP1 KO HEK293 cells (Sayedyahossein et al., 2016) were transiently transfected with an HIV-1-based luciferase reporter vector (pNL4–3.Luc.R-E-), and the cells and the culture supernatants were harvested at 48 h post-transfection. Analysis of the cell lysates using western blot (WB) probed with anti-p24 antisera to detect HIV-1 Gag precursor and mature capsid ($p24^{CA}$) revealed equivalent amounts of intracellular $Pr55^{gag}$ precursor protein in control and IQGAP1-KO cells. Examination of the virion particles pelleted from the culture medium by WB showed a dramatic increase of 12.5-fold ($p = 0.009$) in the levels of $p24^{CA}$ protein released by the IQGAP1-KO cells (Figures 1A and 1B). The increased particle production is consistent with the slight increase of 3.3-fold ($p = 0.03$) in the amount of the cleaved $p24^{CA}$ protein product in the KO cells (Figures 1A and 1B). Luciferase assays from cell lysates revealed no effect of IQGAP1 KO on the expression levels of the luciferase reporter expressed from the Nef open reading frame (ORF) present on the viral vector (Figure 1C), suggesting that IQGAP1 did not affect viral transcription, RNA splicing, or translation but rather affected post-translational Gag functions. To confirm that the increased HIV-1 virus production was attributable to the KO of IQGAP1 and not to off-target effects, we expressed a CRISPR-resistant version of IQGAP1 in the KO cells and again measured the yield of virus produced after transfection with viral DNAs (Figure 1D). Re-introduction of IQGAP1 completely reversed the increase seen in viral particle release in the KO cells back to normal levels of the control cells (Figures 1D and S1A). To test whether the increased viral $p24^{CA}$ levels released into the culture supernatant in IQGAP1-KO cells correlated with an increase in production of infectious virus, we tested the infectivity of the virus harvests. Control and IQGAP1-KO cells were co-transfected as before with the HIV-1-based luciferase reporter vector together with a DNA encoding the vesicular stomatitis virus G envelope glycoprotein (VSV-G). Cells and culture medium were collected at 48 h post-transfection. Cell lysates were tested using WB for the expression of $Pr55^{gag}$ and VSV-G proteins (Figure 1E), and culture supernatants harvested from these cells were used to infect naive HEK293T cells. Luciferase assays of HEK239T cell lysates after infection with virus harvested from IQGAP1-KO cells showed markedly higher levels, ranging from 9-to 12-fold more than the controls ($p < 0.001$ and $p = 0.003$; Figure 1F), indicating that the increased yield of physical particles was matched by a correspondingly increased yield of infectious particles.

These experiments demonstrated the effect of IQGAP1 KO on cells induced to express virus after transfection with HIV-1 DNA. To test whether IQGAP1 has a similar effect on viral release in cells after natural infection with HIV-1 virus, we performed WB analysis of lysates prepared from infected IQGAP1-KO HEK293 cells and their culture supernatants, along with control KO cells. As before, IQGAP1-KO cells infected with HIV-1 had equivalent intracellular $Pr55^{gag}$ expression levels and yet released higher levels of viral $p24^{CA}$ into the culture media compared with the control cells (Figures 1G and S1B).

We next tested the effect of IQGAP1 depletion on virus yield and cellular $Pr55^{gag}$ precursor protein in cells that are more relevant to HIV-1 infection. Stable IQGAP1 KD and control KD lines of Jurkat cells, a human T cell lymphoblast-like cell line, were generated using specific short hairpin RNAs (shRNAs). These lines were infected with the HIV-1 luciferase reporter virus, and cell lysates and culture supernatants were assayed using WB as before. As seen in IQGAP1-KO HEK293 cells, intracellular $Pr55^{gag}$ levels were equivalent for both IQGAP1 and control KD cells, while levels of released viral $p24^{CA}$ were significantly higher in IQGAP1-KD cells (Figures 1H and S1C). Similar data were obtained with infection of primary normal human dermal fibroblasts (NHDFs) after IQGAP1 KD: again the cells expressed equivalent levels of intracellular Gag but produced increased virion yields upon depletion of IQGAP1 (Figure S1D). Altogether, these results demonstrated that for HIV-1, IQGAP1 depletion in a variety of different cell types causes an increase in the production of infectious viral particles.

Overexpression of IQGAP1 Reduces Viral Particles Release

To determine the effect of overexpressing IQGAP1 on HIV-1, HEK293T cells were transiently co-transfected with an HIV-1 luciferase reporter vector (pNL4–3.Luc.R-E-) together with increasing amounts of DNA encoding a GFP-IQGAP1 protein or a DNA expressing GFP or an empty vector DNA as controls. Cells and supernatants were harvested 48 h post-transfection and analyzed for viral proteins using WB. Overexpression of IQGAP1 resulted in a profound dose-dependent decrease in the yield of virions purified from culture supernatant (Figures 2A and 2C). Analysis of cell lysates showed that expression levels of cellular $Pr55^{gag}$ and its cleavage products were unchanged with increasing GFP-IQGAP1 expression levels (Figure 2B). At very high amounts of GFP-IQGAP1 (at a molar ratio of 6:1 GFP-IQGAP1 to HIV-1, producing an 11-fold increase over normal endogenous levels of IQGAP1), we did observe a decrease in the $Pr55^{gag}$ precursor protein and its cleavage products (an average of 2-fold for the $Pr55^{gag}$ precursor and 10-fold for total Gag) without affecting cellular proteins such as GAPDH (Figures 2B and 2C). Overexpression of the GFP alone had no effect (Figures 2B and 2C). As in our IQGAP1 depletion experiments, no difference was observed in the levels of luciferase expressed from the proviral vector in any of the GFP-or GFP-IQGAP1-expressing cells (Figure 2D).

Our experimental system for overexpressing IQGAP1 used a GFP-tagged version of the protein. To confirm that the observed reduction for both HIV-1 cellular Gag expression levels and viral particle release was not due to the GFP tag influencing IQGAP1 functionality, we tested an untagged IQGAP1 expression construct. As in the case of the GFP-tagged IQGAP1, overexpression of untagged IQGAP1 dramatically reduced HIV-1

virion release (Figure S2A). Quantification of the viral particles release revealed a 10-to 22-fold reduction ($p < 0.001$) starting when IQGAP1 was overexpressed at a molar ratio (IQGAP1 to HIV-1) of 4 (Figure S2B). To test whether the effects of IQGAP1 overexpression on virion production are specific to HIV-1, we co-transfected cells with either HIV-1 luciferase reporter vector (pNL4–3.Luc.R-E-) or wild-type (WT) MMuLV DNA (pNCS) together with DNA expressing IQGAP1 or an empty vector control. Forty-eight hours after transfection, the cells and supernatants were analyzed for HIV-1 and MMuLV viral Gags. IQGAP1 overexpression reduced HIV-1 particle release as before and had no effect on MMuLV virion budding (Figure S2C), as previously reported (Leung et al., 2006). Overall, these results demonstrate that IQGAP1 overexpression specifically blocked HIV-1 particle release.

IQGAP1 has been reported to interact with several RNA-binding proteins that participate in mRNA metabolism, including mRNA export factors, mRNA splicing factors, and mRNA splicing regulators (Kristensen et al., 2012; Rosenbluh et al., 2016; Whisenant et al., 2015). The processing and export of HIV-1 Gag mRNA is a complex process that involves avoiding the host cell splicing machinery as well as a unique export of the unsliced viral mRNA using the viral Rev protein and the cell XPO1/CRM1 nuclear export pathway (Fornerod et al., 1997; Fukuda et al., 1997; Malim et al., 1989; Neville et al., 1997; Ossareh-Nazari et al., 1997). Because HIV-1 RNA export and capsid assembly are linked processes (Swanson et al., 2004), the effects on virion production could in principle be mediated by effects on the Rev-dependent export of the Gag mRNA. To test this possibility, we asked whether IQGAP1 overexpression also affects the yield of virion particles resulting from expression of a Rev-independent Gag-Pol construct (Kotsopoulou et al., 2000; Wagner et al., 2000). This construct encodes an mRNA that does not require interaction with the cell splicing machinery and is exported by the global cellular mRNA nucleocytoplasmic export pathway without the assistance of the viral Rev protein (Kotsopoulou et al., 2000; Wagner et al., 2000). HEK293T cells were co-transfected with GFP or an increasing amount of GFP-IQGAP1 together with the codon-optimized Rev-independent Gag-Pol expression vector. VLP release to culture supernatants was decreased (Figure 2E) in a GFP-IQGAP1-dependent manner, just as observed before (Figure 2A). Again, a decrease in intracellular $Pr55^{gag}$ levels was seen only at cells transfected with very high amounts of GFP-IQGAP1 (at molar ratios of GFP-IQGAP1 to pNL4–3.Luc.R-E-of 4 and 6; Figure 2F). These results demonstrate that overexpression of IQGAP1 inhibits the efficient of release of HIV-1 viral particles regardless of the export pathway of the viral Gag mRNA.

We next tested if IQGAP1 overexpression has similar effects on HIV-1 viral particle release from cells resulting from HIV-1 infection rather than transfection. HEK293T cells were transfected with GFP or GFP-IQGAP1, and 1 day post-transfection the cells were infected with HIV-1 at low titer. GFP was monitored using fluorescence-activated cell sorting (FACS) to ensure high transfection efficiency (Figure 2G). Measurement of released $p24^{CA}$ from infected cells overexpressing GFP-IQGAP1 revealed a decrease in HIV-1 virions released to the culture supernatant (Figure 2H), as seen with transfected viral DNA. Overall, these experiment demonstrated that overexpression of IQGAP1 inhibits the efficient release of HIV-1 viral particles regardless of the pathway used to initiate Gag-Pol expression.

Depletion or Overexpression of IQGAP1 Does Not Affect the Viral Early Stages of the Life Cycle

Incoming HIV-1 cores in infected cells are trafficked inward by use of the cellular microtubule network (McDonald et al., 2002). More specifically, we and others previously demonstrated that HIV-1 induces and uses a specific subset of microtubules, stable microtubules, to enhance infection during the viral early stage of the life cycle (Fernandez et al., 2015; Sabo et al., 2013). IQGAP1 interacts with many microtubule-associated proteins (MAPs), including several that have been shown to be important for HIV-1 intracellular movement (Hedman et al., 2015) and are part of the cellular stable microtubule regulatory pathways (Bartolini et al., 2016; Fukata et al., 2002; Tian et al., 2014). To test whether depletion of IQGAP1 affects early steps of viral infection, IQGAP1-KO HEK293 and IQGAP1-KD Jurkat cells were infected with serial dilutions of VSV-G pseudotyped HIV-1 luciferase reporter virus (HIV-1-VSV). Luciferase assays of infected cell lysates at 48 h post-infection revealed no effect of the depletion of IQGAP1 on the early stage of the virus life cycle in either cell type, as demonstrated by equal expression levels of the luciferase reporter (Figures 3A and 3B). To further assure that the luciferase readout from both control and IQGAP1 depleted cells accurately reflect a successful completion of the early stage, resulting in the integration of the provirus into the host genome, we analyzed the integrated proviral DNA copy number in these cells (Figures S3A and S3B). No difference in viral DNA copy number was observed upon IQGAP1 depletion, strengthening the conclusion that the endogenous levels of IQGAP1 do not affect early stages of the HIV-1 life cycle.

HIV-1 virions can infect cells by either membrane fusion at the plasma membrane or after endocytosis (Miyauchi et al., 2009), and HIV-1 vectors can be engineered to use either pathway by pseudotyping with appropriate viral envelope proteins. The VSV-G envelope glycoprotein used to pseudotype HIV-1 virion particles mediates entry via endocytosis (Superti et al., 1987). To test fusion-based entry, we generated HIV-1 luciferase reporter virus pseudotyped with the MMuLV amphotropic envelope (HIV-1-Ampho), which induces fusion at the cell surface (Ragheb et al., 1995). As with HIV-1-VSV, no effect of IQGAP1 depletion on the early stages of the viral life cycle was detected (Figures 3C and 3D).

Next we tested the effect of overexpressing IQGAP1 on the early stages of HIV-1 infection. HEK293T cells were transiently transfected with constructs expressing GFP or GFP-IQGAP1 and infected with serial dilutions of HIV-1-VSV or HIV-1-Ampho as described above. At 48 h post-infection, luciferase assay of cells lysates (Figures 3E and 3F) revealed no effects on the early stages of the virus life cycle upon IQGAP1 overexpression at all virus dilutions. A limitation of overexpressing GFP or GFP-IQGAP1 by transient transfection could be that incoming viruses will infect non-expressing GFP or GFP-IQGAP1 cells in the population. To ensure that only cells that are expressing GFP or GFP-IQGAP1 after transfection are infected, we co-transfected HEK293T cells with GFP or GFP-IQGAP1 DNAs together with a DNA encoding the MMuLV ecotropic receptor mCAT (Yoshimoto et al., 1993) at a ratio of 5:1 (GFP or GFP-IQGAP1 to mCAT; Figure S3C). At 24 h post-transfection, the cells were challenged with serial dilutions of HIV-1 luciferase reporter (HIV-1-Eco) pseudotyped with an MMuLV ecotropic envelope, only mediating entry into

mCAT-expressing cells. Luciferase assay of cells lysates again revealed no effect on the early stage of the virus life cycle upon IQGAP1 overexpression (Figure S3D).

In sum, these results demonstrate that IQGAP1 specifically affects the late stages of HIV-1 life cycle by inhibiting efficient release of progeny virions without any effects on the virus early stages. Thus, IQGAP1 acts as a negative regulator for HIV-1 egress.

The NC and p6 Domains of HIV-1 Gag Interact with IQGAP1

To test whether the inhibition of virus production was mediated by an interaction between IQGAP1 and HIV-1 Gag protein, co-immunoprecipitation (coIP) assays were performed on HEK293T cells co-expressing a WT HIV-1 genome together with GFP-IQGAP1 or control GFP. Immunoprecipitation of the GFP-tagged proteins followed by WB assays for Gag showed that $Pr55^{gag}$ efficiently associated with IQGAP1 but not GFP (Figure 4A). Similar results were obtained when we repeated the coIP experiments in the presence of DNase and RNase, suggesting that the interaction is not mediated by viral or cellular nucleic acids (Figure S4). HIV-1 Gag protein is N-myristoylated, and this post-translational modification plays an important role in targeting the protein to the cell plasma membrane that serves as the budding site for HIV-1 (Bouamr et al., 2003; Bryant and Ratner, 1990; Ono and Freed, 1999; Saad et al., 2007; Zhou and Resh, 1996). To test whether the interaction between IQGAP1 and HIV-1 Gag depends on the ability of Gag to reach the plasma membrane, we tested the binding to a Gag mutant that is not myristoylated by virtue of a change of the N-terminal glycine to alanine (G2A). coIP experiments revealed that even when Gag cannot be targeted to the plasma membrane, it still retained its interaction with IQGAP1 (Figure 4B).

HIV-1 $Pr55^{gag}$ protein is processed to form six mature proteins, each with a distinct functionality (Scarlata and Carter, 2003). To test which portions of the Gag precursor mediate the interaction with IQGAP1, we created a series of flag-tagged Rev-independent Gag expression constructs encoding the MA protein and increasing numbers of the downstream proteins (Figure 4C). These constructs were then used in coIP assays as before. Once the NC domain was present in the transfected DNA constructs, Gag was able to efficiently bind IQGAP1 (Figure 4D). To further test whether additional Gag domains downstream of NC might also mediate the interaction with IQGAP1 independently of the NC-mediated binding observed above, we generated an additional construct lacking the NC domain (GagDNC; Figure 4C). coIP assays demonstrated that the p6 domain of Gag also facilitates an interaction with IQGAP1 (Figure 4E). These findings showed the C terminus region of HIV-1 Gag protein is important for the interaction with IQGAP1 and that either the NC or the p6 domains was sufficient to mediate this interaction.

Interaction of IQGAP1 with the C Terminus Region of HIV-1 Gag Is Required for Negatively Regulating Virion Production Independently of Gag L Domains

We sought to test if IQGAP1's ability to negatively regulate HIV-1 viral release depended on its interaction with the C terminus region of Gag. We generated a Rev-independent flag-tagged HIV-1 Gag construct in which the C terminus region, including NC and the p6 domain, was replaced with the leucine zipper domain of the yeast transcription factor GCN4 (GagZ-flag; Figure 5A). This replacement was demonstrated previously to support the

efficient release of HIV-1 VLPs in the absence of the NC and p6 (Accola et al., 2000). HEK293T cells were co-transfected with either WT flag-tagged Gag (Gag-flag; Figure 5A) or the GagZ-flag construct together with increasing amounts of GFP-IQGAP1 expression plasmid or GFP control. No reduction in the amount of released VLPs could be detected by WB in supernatants from cells transfected with the GagZ-flag construct (Figures 5C and S5A), even at a very high amount of transfected GFP-IQGAP1 DNA (Figure S5B). In contrast, as observed previously (Figure 2), cells expressing Gag-flag demonstrated a marked dose-dependent decrease in the yield of VLPs (Figures 5B and S5A). These results demonstrate that IQGAP1 interaction with Gag is essential for its inhibitory effect.

Next, we tested whether both the NC and p6 domains of the Gag protein, which can independently interact with IQGAP1, are required for regulation by IQGAP1. Flag-tagged HIV-1 Gag constructs with deletion of either the p6 domain (GagDp6-flag; Figure 5A) or the NC domain (GagΔDNC-flag; Figure 5A) were generated, and HEK293T cells were co-transfected with these DNAs together with increasing amounts of GFP-IQGAP1 or GFP control as before. As described in previous studies (Dawson and Yu, 1998; Göttlinger et al., 1991; Zhang and Barklis, 1997), both constructs displayed defective Gag assembly and a significant decrease in VLP production compared with WT Gag-flag, but VLPs could still be detected (Figures S5C and S5D). Upon overexpression of GFP-IQGAP1, cells transfected with WT Gag-flag or either of the gag mutants (GagDNC-flag and Gag-Dp6-flag) displayed a marked decrease of VLP production in a dose-dependent manner (Figures 5B, 5D, 5E, and S5A). These results show that either one of the two IQGAP1-interacting domains in the C terminus region of HIV-1 Gag is sufficient for IQGAP1 to perform its negative regulation.

The p6 domain of HIV-1 Gag contains two late-domain sequences, a PTAP and LYP$(X)_n$L motifs. These sequences mediate Gag interactions with components of the cellular ESCRT machinery, the TSG101 and Alix proteins, which significantly enhance virus budding (Sundquist and Kräusslich, 2012). The NC domain of Gag has been also shown to contribute to the interactions between the p6 late-domain sequences and the TSG101 and Alix proteins (Chamontin et al., 2015; Dussupt et al., 2009). We next asked if IQGAP1's negative regulation of HIV-1 release requires Gag to interact with the ESCRT machinery. We mutated each of the two putative late-domains sequences in the p6 domain of our flag-tagged Gag expression construct, changing critical residues to alanine (Figure 5F). As in the case of deleting the p6 domain (Figure S5C), these late domains mutations caused a severe defect in viral release, though VLPs could still be detected (Figure S5E). The constructs were then co-transfected with increasing amounts of GFP-IQGAP1 or a GFP control DNA and tested for the effect on viral release. Gag mutants with changes in either one of the late domains were still strongly affected by IQGAP1 overexpression, similar to the parental WT Gag construct (Figures 5G–5I and S5F). Next, we tested if completely abolishing Gag's ability to interact with the ESCRT machinery can prevent further downregulation of virion production by IQGAP1 overexpression. We generated a double mutant with alteration of both late domains (Figure 5F) and tested it as before. Even when both late domains were mutated, IQGAP1 overexpression severely reduced the residual basal VLP release (Figures 5J and S5F), as observed for WT Gag (Figure 5G). Altogether, these results demonstrated that IQGAP1's negative regulation of HIV-1 viral release is independent of the ability of Gag to recruit the

ESCRT machinery and suggest that IQGAP1 inhibition of virion release depends on its interaction with Gag.

IQGAP1 Restricts HIV-1 Gag Targeting to the Plasma Membrane

The two opposing effects of depletion and overexpression of IQGAP1 on HIV-1 particle release could be mediated by altering the subcellular localization of Gag. To address this possibility, we examined Gag cellular distribution in both scenarios. We first tested Gag localization in cells overexpressing IQGAP1. HEK293T cells were co-transfected with an HIV-1 genome expressing luciferase together with GFP-IQGAP1 or control GFP expression constructs. At 48 h post-transfection, cells were lysed and luciferase levels were measured to ensure equal transfection levels of the HIV-1 reporter virus (Figure S6A). In parallel, the cells were fixed, stained for HIV-1 Gag and imaged using confocal microscopy. Control GFP-expressing cells displayed a characteristic punctate pattern of Gag staining (Figure 6A), while cells expressing GFP-IQGAP1 exhibited a diffuse cytoplasmic Gag stain and a dramatic reduction in Gag punctate staining (Figure 6A). We detected equivalent luciferase levels between these cells (Figure S6A) as well as equivalent levels of cell viability measured by trypan blue assay (data not shown). Additionally, cells transfected with either GFP or GFP-IQGAP1 displayed intact microtubule staining (Figure S6B), suggesting no major restructuring of the cytoskeleton, though cells overexpressing GFP-IQGAP1 displayed a more rounded morphology compared with GFP-expressing cells. To verify the relocalization of Gag by a different method, we prepared gentle lysates, separated membrane and cytosolic fractions by membrane floatation, and measured Gag levels using WB (Figure 6B). Quantification (Figure 6C) revealed a large decrease ($p = 0.0015$) in the levels of membrane-associated Gag in GFP-IQGAP1-expressing cells compared with GFP controls, consistent with the Gag immunofluorescence findings.

Gag localization was also assessed after IQGAP1 depletion. HEK293 IQGAP1-KO and control cells were transfected with an HIV-1 genome expressing luciferase as before, and 48 h post-transfection, the cells were lysed to measure luciferase levels (Figure S7) or fixed, stained for HIV-1 Gag, and examined using confocal imaging. The IQGAP1-KO cells exhibited significantly increased punctate Gag staining and a stronger Gag association with the plasma membrane, the sites for virion budding (Figure 7A). Gag expression levels in membrane fractions collected by floatation and assessed using WB revealed a significant increase ($p < 0.001$) in membrane-associated Gag in IQGAP1-KO cells compared with control cells (Figures 7B and 7C). Overall, these experiments suggest that the changes in viral particles release when IQGAP1 is overexpressed or depleted is associated with marked changes in the steady-state distribution of cellular Gag near the cellular plasma membrane.

DISCUSSION

We have identified IQGAP1 as a negative regulator of HIV-1 viral egress that acts to reduce the accumulation of the viral structural protein, the Gag protein, at the cell plasma membrane. IQGAP1 KO increased the yield of viral particles (Figure 1), while overexpression diminished viral progeny production (Figure 2). These results show that even at its endogenous expression levels, IQGAP1 acts to limit HIV-1 viral particle release. It

should be noted that IQGAP1 is a ubiquitously expressed gene found in many cell types, including T cells and macrophages, that are relevant to HIV-1 infection (Abel et al., 2015; Smith et al., 2015; White et al., 2012). Thus, this host protein may be limiting virus spread *in vivo*.

IQGAP1 participates in many cytoskeletal regulatory pathways (Abel et al., 2015; Briggs and Sacks, 2003; Mateer et al., 2003; Noritake et al., 2005; Watanabe et al., 2015; White et al., 2012). One of these regulated pathways is the formation of stabilized detyrosinated microtubules (Bartolini et al., 2016). To enhance its infection, HIV-1 actively induces the formation of stable microtubules, including detyrosinated and acetylated microtubules (Sabo et al., 2013). Nevertheless, we found no evidence of IQGAP1 affecting the early stages of the virus life cycle (Figure 3). Our data clearly show that the negative regulation of IQGAP1 on HIV-1 life cycle was taking place only during the late stages. Thus, our results suggest that HIV-1 infection can overcome any need for IQGAP1 in using stable microtubules during the early phases of infection.

The involvement of IQGAP1 as a host factor essential for budding and release of several enveloped viruses has been previously noted (Dolnik et al., 2014; Gladue et al., 2011; Lu et al., 2013). As a regulator of many cellular processes, IQGAP1 can either be a positive or a negative regulator for other non-viral intracellular pathogens (Hedman et al., 2015; Kim et al., 2011; Lu et al., 2015; Simon et al., 2015). Our findings demonstrating that IQGAP1 is a negative factor for HIV-1 are in line with the dual roles of IQGAP1. This dual role is exemplified by the observation that for MMuLV, a close relative of HIV-1, IQGAP1 was shown to be an essential factor assisting viral spread in culture (Leung et al., 2006). Mouse and human IQGAP1 are 94% identical (Briggs and Sacks, 2003), and it is unlikely that the different effects on viral release observed for HIV-1 compared with MMuLV is due to the small differences in the sequence of the IQGAP1 protein. Rather, it is more likely that these viruses evolved to make distinctive use of the IQGAP1 host factor for the completion of their late stage. Analogous differences can be seen in the different ESCRT recruitment needs between these viruses (Demirov and Freed, 2004; Morita and Sundquist, 2004).

IQGAP1 is a scaffold protein that interacts with a large number of cellular and non-cellular proteins (Abel et al., 2015; Hedman et al., 2015; White et al., 2012). It is notable that it interacts with two separate domains within the HIV-1 Gag protein: the p6 and NC domains (Figure 4). Importantly, interaction of IQGAP1 with either the p6 or the NC domains in Gag is sufficient to allow IQGAP1 to negatively regulate HIV-1 particle release (Figure 5). The replacement of both domains with the leucine zipper domain of the yeast transcription factor GCN4 completely eliminated restriction (Figure 5), indicating that there are no other regions of Gag that are targeted by IQGAP1. This result also shows that the assembly and release of virions per se is not affected by IQGAP1: only Gags that retain the interaction domains with IQGAP1 are subject to the restriction. The evolution of two separate interactions between IQGAP1 and HIV-1 Gag, each by itself sufficient to support IQGAP1 negative regulation of viral release, suggests that IQGAP1 negative regulation on viral release is important for either the virus or the host.

The p6 and NC domains that interact with IQGAP1 have been shown to be important for the ability of the virus to recruit the ESCRT machinery needed for efficient completion of the late stages of the virus life cycle (Demirov and Freed, 2004; Morita and Sundquist, 2004). The recruitment of ESCRT is achieved by binding the TSG101 and Alix proteins, both part of ESCRT, to the specific L domains within Gag (Henne et al., 2011; Schmidt and Teis, 2012). Our results demonstrating that IQGAP1 inhibits HIV-1 budding independently of the Gag late domains (Figure 5) but requiring interaction with Gag suggests that its activity is mediated by directly targeting Gag. Nevertheless, it should be noted that IQGAP1 has been shown to also interact with TSG101 and Alix (Morita et al., 2007). This raises the possibility that although the IQGAP1 effects on Gag do not require the L domains, the negative regulation of HIV-1 viral release might still involve the ESCRT machinery functionality through IQGAP1 interaction with that machinery.

IQGAP1 interacts with many plasma membrane-associated molecules (Hedman et al., 2015; Smith et al., 2015; White et al., 2012). Specifically, IQGAP1 was shown participate in the active removal of several membrane proteins from the cell surface using the endocytic pathway in order to recycle them (Bamidele et al., 2015; Ghosh et al., 2019; Liu et al., 2013). Our data demonstrated that IQGAP1 can interact with membrane-bound myristylated Gag as well as with cytoplasmic unmyristylated Gag (Figure 4). Taken together, a plausible explanation for the reduction in the accumulation levels of Gag proteins at the plasma membrane (Figure 6) is that IQGAP1 is actively removing Gag proteins from the plasma membrane as well as preventing cytoplasmic Gag from trafficking to it. It is intriguing to hypothesize that HIV-1 may have evolved to use IQGAP1 as a means to control the amount of viral release from infected cells. Limiting the amount of Gag budding at the plasma membrane may prolong the amount of time that the cell can be used to produce viral particles. As has been proposed for other negative regulators of Gag function, this may allow time for the appropriate levels of the Envelope protein to be delivered to the site of budding and incorporated into the nascent virion particle (Mu et al., 2015).

In conclusion, we have here identified IQGAP1 as an HIV-1-interacting protein that negatively regulates viral particle release. We have characterized Gag interaction domains with IQGAP1 and demonstrated the mode of action by which IQGAP1 affects HIV-1 budding. Our findings that IQGAP1 limits the presence of Gag proteins at the cellular plasma membrane are the first example of a viral structural protein being negatively regulated by IQGAP1 and further demonstrate IQGAP1's broad regulatory roles in diverse cellular processes, including the regulation of cellular membrane-bound proteins.

STAR★METHODS

LEAD CONTACT AND MATERIALS AVAILABILITY

Further information and requests for resources and reagents should be directed to and will be fulfilled by the Lead Contact, Stephen P. Goff (spg1@cumc.columbia.edu).

METHOD DETAILS

DNA Constructs—The GFP-expressing plasmid DNA pEGFP-C1 was purchased from Clontech (Cat# 6085–1). pEGFP-IQGAP1 was a gift from David Sacks (Addgene plasmid # 30112; [Ren et al., 2005]). pNL4–3.Luc.E-.R-was acquired from the AIDS Reagent Repository (Cat# 3418; [Connor et al., 1995]). pHA-mCAT was a gift from Walther Mothes (Yale University School of Medicine). pNCS, which encodes a full-length clone of MMuLV, was described elsewhere (Yueh and Goff, 2003). To generate an untagged IQGAP1 expression construct (pCDNA4-IQGAP1), pEGFP-IQGAP1 and pCDNA4/TO (ThermoFisher; Cat# V102020) were digested using XhoI and XbaI (NEB; Cat# R0146 and R0145) restriction enzymes. The IQGAP1 fragment and the pCDNA4/TO vector were gel purified using QIAGEN QIAquick Gel Extraction Kit (-QIAGEN; Cat# 28706) and ligated to create the pCDNA-4/TO-IQGAP1 plasmid. CRISPR-resistant pEGFP-IQGAP1 (pEGFP-IQGAP1-XPR-res) was generated by digesting the IQGAP1-XPR-res fragment (IDT; Table S1) with XhoI and XmnI restriction enzymes (NEB; Cat# R0146 and R0194) and ligating it into pEGFP-IQGAP1 plasmid that was digested using the same restriction enzymes. Untagged CRISPR-resistant IQGAP1 expression construct (pCDNA4-IQGAP1-XPR-res) was generated using the same method described above for the untagged-IQGAP1 expression vector using the pEGFP-IQGAP1-XPR-res and pCDNA4/TO plasmids. Empty vector control for experiments that used pEGFP-IQGAP1 was generated by digesting pEGFP-C1 with AfeI and SmaI (NEB; Cat# R0652 and R0141), gel purification with QIAGEN QIAquick Gel Extraction Kit and self-ligation of the digested vector. pCDNA4/TO served as an empty vector for experiments conducted with the pCDNA4-IQGAP1 or pCDNA4-IQGAP1-XPR-res plasmids. Gag G2A was generated by overlapping PCR using the pNL4–3.Luc.E-.R-plasmid and HIV-1 PauI FW together with MA G2A REV primers and with MA G2A FW together with HIV-1 SpeI REV primers. The second PCR using HIV-1 PauI FW together with HIV-1 SpeI REV primers was digested using PauI and SpeI (NEB; Cat# R0651 and R0133) and ligated into the parental pNL4–3.Luc.E-.R-plasmid that was digested using the same restriction enzymes. Flag-tagged Rev-independent HIV-1 Gag domain expression constructs were purchased as gBlocks (IDT; Table S1), digested using KpnI and XhoI (NEB; Cat# R3142 and R0146; respectively) and ligated into pCDNA4/TO, which was digested using the same restriction enzymes. $PTAP_{mut}$ plasmid was generated by overlapping PCR using the Gag-flag plasmid and REVi Gag FW together with PTAP2AAA REV primers and REVi Gag REV together with PTAP2AAA FW primers. $LYPXnL_{mut}$ plasmid was generated by PCR using the Gag-flag plasmid and the REVi Gag Fw and YPXL2AAAA REV primers. PTAP/$LYPXnL_{mut}$ was generated using the PTAPmut plasmid and the cloning primer of $LYPXnL_{mut}$. All PCR fragments were cloned into pcDNA4/TO as described above. All constructs were verified by sequencing using CMV FW and BGH REV primers. All primers are listed in Table S2.

Cells—IQGAP1 KO and control HEK293 cells were kindly provided by Dr. David B. Sacks (NIH; [Sayedyahossein et al., 2016]). NHDFs were purchased from Lonza (Cat# CC-2509). HEK293T cells were purchased from ATCC (Cat# CRL-11268). All cells described above were maintained in Dulbecco's Modified Eagle Medium supplemented with 10% fetal bovine serum, 2 mM l-glutamine (GIBCO, Cat# 25030–164), 100 U/ml penicillin and 100 μg/ml streptomycin (GIBCO, Cat# 15140–163). Jurkat cells were purchased from

ATCC (Cat# TIB-152) and were maintained in in RPMI-1640 medium with 10% fetal bovine serum, 2 mM l-glutamine, 100 U/ml penicillin and 100 μg/ml streptomycin. Jurkat cells which stably express scrambled shRNA or two different shRNAs against IQGAP1 were generated by infecting these cells with VSV-G pseudotyped pLKO based scrambled and IQGAP1 shRNAs lentiviral vectors (Dharmacon: Cat# RHS6848, Cat# TRCN0000047483 and Cat# TRCN0000047485). Follow infection, the cells were selected and pooled in medium with 1 μg/ml puromycin.

Quantitative Measurement of HIV-1 $p24^{CA}$—Quantitative measurement of HIV-1 $p24^{CA}$ levels in culture supernatants was performed using Abcam HIV-1 p24 SimpleStep ELISA Kit (Abcam, Cat# ab218268) according to the manufacturer instructions.

Cells Viability Assay—Cells viability was assed using 0.4% Trypan Blue Solution (ThermoFisher; Cat# 15250061) according to the manufacturer instructions.

Transfection, Virus Preparation, and Infection—Plasmids transfections were performed using lipofectamine 2000 (ThermoFisher; Cat# 11668019) according to the manufacturer's instruction. All transfections were performed in six-well plates unless otherwise noted. The amounts of DNA used in each experiment is given in the figure legends. VSV-G, MuLV amphotropic or MuLV ecotropic pseudotyped HIV-1 luciferase viruses were generated by co-transfecting HEK293T cells in 10-cm dishes with either pVSV-G, pHIT123 or pHIT456 together with pNL4–3.Luc.E-.R-(AIDS Reagent Repository number 3418; [Connor et al., 1995]). After 48 h, virus in media was collected and filtered through a 0.45 μm membrane and stored at —80°C. Unless otherwise indicated, viral infections were carried out for 2 h in the presence of 4 mg/mL polybrene (Millipore Sigma; Cat# TR-1003-G) after which the cells were washed once with PBS and fresh media was added.

siRNA transfection—IQGAP1 and non-targeting control siRNAs were obtained from Dharmacon (SMARTpool: ON-TARGETplus siRNA Cat# L-004694–00-0005 and D-001810–10). All siRNA transfection were performed in six-well plates using Lipofectamine RNAiMAX Transfection Reagent according to the manufacturer's instructions.

Luciferase assay—Luciferase activity was assayed using Promega Luciferase Assay System (Cat# E4550).

Western blots—Unless otherwise indicated, cells were lysed in CelLytic M Cell Lysis Reagent (Sigma; Cat# C2978) for 30 min at 4°C. The lysate was then cleared from cellular debris by centrifugation for 15 min at 13000 rpm at 4°C, and 4x Laemmli Sample Buffer (BIO-RAD; Cat# 161–0747) supplemented with 20% β-Mercaptoethanol was added to the clear supernatant to a final concentration of 1x. Samples were then heated briefly at 100°C. Proteins were resolved by SDS-PAGE electrophoresis, transferred to a PVDF membrane (Millipore Sigma; Cat# IPFL00010) and probed by western blotting. Antibodies used are listed in Table S3. Densitometric quantification was performed using ImageJ and the relative band intensity was normalized against GAPDH.

Co-Immunoprecipitation—Cells were lysed in 0.5% NP40 Lysis buffers (50 mM Tris pH 7.5, 150 mM NaCl, 0.5% NP40) for 30 min at 4°C. The lysate was cleared from cellular debris by centrifugation for 15 min at 13000 rpm at 4°C. Clear supernatant was mixed with anti-GFP magnetic beads (MBL; Cat# D153–11) and the mixture was incubated at 4°C for 4 h. The beads were washed three times with buffer (50 mM Tris pH 7.5, 150 mM NaCl, 0.1% NP40) and the proteins bound to the beads were recovered and detected by western blotting using specific antibodies. In some experiments samples were treated to remove DNA and RNA, utilizing DNase (Promega; Cat# M6101) and RNase (ThermoFisher; Cat# AM2271) added to the lysing buffer, with an additional 1 hour incubation at room temperature prior to clearing the cellular debris.

Membrane Floatation Assay—Membrane floatation assays were performed as described before (Ono and Freed, 1999) with minor modifications. Briefly, 5×10^6 cells were washed twice in buffer [10 mM Tris-HCl (pH 7.5), 1 mM EDTA and 1 mM EGTA], scraped into 1 mL homogenization buffer [10 mM Tris-HCl (pH 7.5), 1 mM EDTA, 10% sucrose, supplemented with protease inhibitor cocktail] and incubated for 10 minutes on ice. Cell suspensions were subjected to 30 strokes in a Dounce homogenizer and nuclei were pelleted by centrifugation at 500 x g for 5 min at 4°C. Clear 250 mL of postnuclear extract was mixed with 1.25 mL of 85.5% sucrose in TE buffer [10 mM Tris pH 8.0, 1 mM EDTA] and placed at the bottom of a 12 mL SW41 (Beckman Coulter; Cat# 331372) ultracentrifuge tube. A discontinuous step gradient was formed above the cell extracts by adding 7 mL of 65% sucrose in TE and 3 mL of 10% sucrose in TE and the samples were centrifuged at 100,000 × g for 18 h at 4°C (SW41 rotor, Beckman). Ten 1.2ml fractions were collected from the top of the gradient and total proteins from each fraction were recovered using TCA precipitation.

Immunostaining and Microscopy—Cells grown on glass coverslips were fixed with ice-cold methanol for 5 min following blocking and permeabilization with PBS supplemented with 2% BSA, 10% FBS, and 0.3% Triton X-100 for 30 minutes. Samples were then incubated with primary antibody in PBS supplemented with 1% BSA for 2 h, washed three times in PBS and incubated with the appropriate Alexa Fluor-conjugated secondary in PBS for 1 hour at room temperature. Cell nuclei were stained using 4,6-diamidino-2-phenylindole (DAPI; 1 μg/mL, Sigma, D9564–10MG) dissolved in PBS for 20 minutes at room temperature. Coverslips were then washed three times in PBS and mounted using FluorSave mounting medium (Millipore Sigma; Cat# 345789–20ML). Images were acquired using motorized spinning-disc confocal microscope (Yokogawa CSU-X1 A1 confocal head and Zeiss Axio Observer Z1 microscope) and SlideBook Software (Intelligent Imaging Innovations). Antibodies used are listed in Table S3.

Genomic DNA extraction and Quantitative PCR—Genomic DNA extraction was performed using DNeasy Blood and Tissue Kit (Qiagne; Cat# 69506) according to the manufacturer's instructions. Quantitative PCR (qPCR) was performed in an ABI 7500 Fast Real-Time PCR machine using FastStart Universal SYBR Green Master (Rox) (Millipore Sigma; Cat# 4913850001). qPCR primers are listed in Table S2.

QUANTIFICATION AND STATISTICAL ANALYSIS

Sample size is provided in the figure legends. Statistical significance was determined by two-tailed Student's t test. Results are presented as the average ± SEM.

Supplementary Material

Refer to Web version on PubMed Central for supplementary material.

ACKNOWLEDGMENTS

S.P.G. is a Howard Hughes Medical Institute (HHMI) investigator. This study was supported in part by a grant from the NIH, United States (R01 CA 030488).

REFERENCES

Abel AM, Schuldt KM, Rajasekaran K, Hwang D, Riese MJ, Rao S, Thakar MS, and Malarkannan S (2015). IQGAP1: insights into the function of a molecular puppeteer. Mol. Immunol 65, 336–349. [PubMed: 25733387]

Accola MA, Strack B, and Göttlinger HG (2000). Efficient particle production by minimal Gag constructs which retain the carboxy-terminal domain of human immunodeficiency virus type 1 capsid-p2 and a late assembly domain. J. Virol 74, 5395–5402. [PubMed: 10823843]

Bamidele AO, Kremer KN, Hirsova P, Clift IC, Gores GJ, Billadeau DD, and Hedin KE (2015). IQGAP1 promotes CXCR4 chemokine receptor function and trafficking via EEA-1+ endosomes. J. Cell Biol 210, 257–272. [PubMed: 26195666]

Bartolini F, Andres-Delgado L, Qu X, Nik S, Ramalingam N, Kremer L, Alonso MA, and Gundersen GG (2016). An mDia1-INF2 formin activation cascade facilitated by IQGAP1 regulates stable microtubules in migrating cells. Mol. Biol. Cell 27, 1797–1808. [PubMed: 27030671]

Bouamr F, Scarlata S, and Carter C (2003). Role of myristylation in HIV-1 Gag assembly. Biochemistry 42, 6408–6417. [PubMed: 12767222]

Briggs MW, and Sacks DB (2003). IQGAP proteins are integral components of cytoskeletal regulation. EMBO Rep 4, 571–574. [PubMed: 12776176]

Bryant M, and Ratner L (1990). Myristoylation-dependent replication and assembly of human immunodeficiency virus 1. Proc. Natl. Acad. Sci. U S A 87, 523–527. [PubMed: 2405382]

Chamontin C, Rassam P, Ferrer M, Racine PJ, Neyret A, Lainé S, Milhiet PE, and Mougel M (2015). HIV-1 nucleocapsid and ESCRT-component Tsg101 interplay prevents HIV from turning into a DNA-containing virus. Nucleic Acids Res 43, 336–347. [PubMed: 25488808]

Chertova E, Chertov O, Coren LV, Roser JD, Trubey CM, Bess JW Jr., Sowder RC 2nd, Barsov E, Hood BL, Fisher RJ, et al. (2006). Proteomic and biochemical analysis of purified human immunodeficiency virus type 1 produced from infected monocyte-derived macrophages. J. Virol 80, 9039–9052. [PubMed: 16940516]

Choi S, and Anderson RA (2016). IQGAP1 is a phosphoinositide effector and kinase scaffold. Adv. Biol. Regul 60, 29–35. [PubMed: 26554303]

Christ L, Raiborg C, Wenzel EM, Campsteijn C, and Stenmark H (2017). Cellular functions and molecular mechanisms of the ESCRT membrane-scission machinery. Trends Biochem. Sci 42, 42–56. [PubMed: 27669649]

Connor RI, Chen BK, Choe S, and Landau NR (1995). Vpr is required for efficient replication of human immunodeficiency virus type-1 in mononuclear phagocytes. Virology 206, 935–944. [PubMed: 7531918]

Dawson L, and Yu XF (1998). The role of nucleocapsid of HIV-1 in virus assembly. Virology 251, 141–157. [PubMed: 9813210]

Demirov DG, and Freed EO (2004). Retrovirus budding. Virus Res 106, 87–102. [PubMed: 15567490]

Dolnik O, Kolesnikova L, Welsch S, Strecker T, Schudt G, and Becker S (2014). Interaction with Tsg101 is necessary for the efficient transport and release of nucleocapsids in marburg virus-infected cells. PLoS Pathog 10, e1004463. [PubMed: 25330247]

Dussupt V, Javid MP, Abou-Jaoudé G, Jadwin JA, de La Cruz J, Nagashima K, and Bouamr F (2009). The nucleocapsid region of HIV-1 Gag cooperates with the PTAP and LYPXnL late domains to recruit the cellular machinery necessary for viral budding. PLoS Pathog 5, e1000339. [PubMed: 19282983]

Fackler OT, and Kräusslich HG (2006). Interactions of human retroviruses with the host cell cytoskeleton. Curr. Opin. Microbiol 9, 409–415. [PubMed: 16820319]

Fernandez J, Portilho DM, Danckaert A, Munier S, Becker A, Roux P, Zambo A, Shorte S, Jacob Y, Vidalain PO, et al. (2015). Microtubule-associated proteins 1 (MAP1) promote human immunodeficiency virus type I (HIV-1) intracytoplasmic routing to the nucleus. J. Biol. Chem 290, 4631–4646. [PubMed: 25505242]

Fornerod M, Ohno M, Yoshida M, and Mattaj IW (1997). CRM1 is an export receptor for leucine-rich nuclear export signals. Cell 90, 1051–1060. [PubMed: 9323133]

Fukata M, Watanabe T, Noritake J, Nakagawa M, Yamaga M, Kuroda S, Matsuura Y, Iwamatsu A, Perez F, and Kaibuchi K (2002). Rac1 and Cdc42 capture microtubules through IQGAP1 and CLIP-170. Cell 109, 873–885. [PubMed: 12110184]

Fukuda M, Asano S, Nakamura T, Adachi M, Yoshida M, Yanagida M, and Nishida E (1997). CRM1 is responsible for intracellular transport mediated by the nuclear export signal. Nature 390, 308–311. [PubMed: 9384386]

Garrus JE, von Schwedler UK, Pornillos OW, Morham SG, Zavitz KH, Wang HE, Wettstein DA, Stray KM, Côté M, Rich RL, et al. (2001). Tsg101 and the vacuolar protein sorting pathway are essential for HIV-1 budding. Cell 107, 55–65. [PubMed: 11595185]

Ghosh M, Lo R, Ivic I, Aguilera B, Qendro V, Devarakonda C, and Shapiro LH (2019). CD13 tethers the IQGAP1-ARF6-EFA6 complex to the plasma membrane to promote ARF6 activation, b1 integrin recycling, and cell migration. Sci. Signal 12, eaav5938. [PubMed: 31040262]

Gladue DP, Holinka LG, Fernandez-Sainz IJ, Prarat MV, O'Donnell V, Vepkhvadze NG, Lu Z, Risatti GR, and Borca MV (2011). Interaction between Core protein of classical swine fever virus with cellular IQGAP1 protein appears essential for virulence in swine. Virology 412, 68–74. [PubMed: 21262517]

Göttlinger HG, Sodroski JG, and Haseltine WA (1989). Role of capsid precursor processing and myristoylation in morphogenesis and infectivity of human immunodeficiency virus type 1. Proc. Natl. Acad. Sci. U S A 86, 5781–5785. [PubMed: 2788277]

Göttlinger HG, Dorfman T, Sodroski JG, and Haseltine WA (1991). Effect of mutations affecting the p6 gag protein on human immunodeficiency virus particle release. Proc. Natl. Acad. Sci. U S A 88, 3195–3199. [PubMed: 2014240]

Hedman AC, Smith JM, and Sacks DB (2015). The biology of IQGAP proteins: beyond the cytoskeleton. EMBO Rep 16, 427–446. [PubMed: 25722290]

Henne WM, Buchkovich NJ, and Emr SD (2011). The ESCRT pathway. Dev. Cell 21, 77–91. [PubMed: 21763610]

Hurley JH, and Hanson PI (2010). Membrane budding and scission by the ESCRT machinery: it's all in the neck. Nat. Rev. Mol. Cell Biol 11, 556–566. [PubMed: 20588296]

Kim H, White CD, and Sacks DB (2011). IQGAP1 in microbial pathogenesis: targeting the actin cytoskeleton. FEBS Lett 585, 723–729. [PubMed: 21295032]

Kotsopoulou E, Kim VN, Kingsman AJ, Kingsman SM, and Mitrophanous KA (2000). A Rev-independent human immunodeficiency virus type 1 (HIV-1)-based vector that exploits a codon-optimized HIV-1 gag-pol gene. J. Virol 74, 4839–4852. [PubMed: 10775623]

Kristensen AR, Gsponer J, and Foster LJ (2012). A high-throughput approach for measuring temporal changes in the interactome. Nat. Methods 9, 907–909. [PubMed: 22863883]

Leung J, Yueh A, Appah FS Jr., Yuan B, de los Santos K, and Goff SP (2006). Interaction of Moloney murine leukemia virus matrix protein with IQGAP. EMBO J 25, 2155–2166. [PubMed: 16628219]

Liu C, Billadeau DD, Abdelhakim H, Leof E, Kaibuchi K, Bernabeu C, Bloom GS, Yang L, Boardman L, Shah VH, and Kang N (2013). IQGAP1 suppresses TbβII-mediated myofibroblastic activation and metastatic growth in liver. J. Clin. Invest 123, 1138–1156. [PubMed: 23454766]

Lu J, Qu Y, Liu Y, Jambusaria R, Han Z, Ruthel G, Freedman BD, and Harty RN (2013). Host IQGAP1 and Ebola virus VP40 interactions facilitate virus-like particle egress. J. Virol 87, 7777–7780. [PubMed: 23637409]

Lu R, Herrera BB, Eshleman HD, Fu Y, Bloom A, Li Z, Sacks DB, and Goldberg MB (2015). Shigella effector OspB activates mTORC1 in a manner that depends on IQGAP1 and promotes cell proliferation. PLoS Pathog 11, e1005200. [PubMed: 26473364]

Malim MH, Böhnlein S, Hauber J, and Cullen BR (1989). Functional dissection of the HIV-1 Rev trans-activator–derivation of a trans-dominant repressor of Rev function. Cell 58, 205–214. [PubMed: 2752419]

Martin-Serrano J, Zang T, and Bieniasz PD (2001). HIV-1 and Ebola virus encode small peptide motifs that recruit Tsg101 to sites of particle assembly to facilitate egress. Nat. Med 7, 1313–1319. [PubMed: 11726971]

Mateer SC, Wang N, and Bloom GS (2003). IQGAPs: integrators of the cytoskeleton, cell adhesion machinery, and signaling networks. Cell Motil. Cytoskeleton 55, 147–155. [PubMed: 12789660]

McDonald D, Vodicka MA, Lucero G, Svitkina TM, Borisy GG, Emerman M, and Hope TJ (2002). Visualization of the intracellular behavior of HIV in living cells. J. Cell Biol 159, 441–452. [PubMed: 12417576]

Miyauchi K, Kim Y, Latinovic O, Morozov V, and Melikyan GB (2009). HIV enters cells via endocytosis and dynamin-dependent fusion with endosomes. Cell 137, 433–444. [PubMed: 19410541]

Morita E, and Sundquist WI (2004). Retrovirus budding. Annu. Rev. Cell Dev. Biol 20, 395–425. [PubMed: 15473846]

Morita E, Sandrin V, Chung HY, Morham SG, Gygi SP, Rodesch CK, and Sundquist WI (2007). Human ESCRT and ALIX proteins interact with proteins of the midbody and function in cytokinesis. EMBO J 26, 4215–4227. [PubMed: 17853893]

Mu X, Fu Y, Zhu Y, Wang X, Xuan Y, Shang H, Goff SP, and Gao G (2015). HIV-1 exploits the host factor RuvB-like 2 to balance viral protein expression. Cell Host Microbe 18, 233–242. [PubMed: 26211835]

Naghavi MH, and Goff SP (2007). Retroviral proteins that interact with the host cell cytoskeleton. Curr. Opin. Immunol 19, 402–407. [PubMed: 17707624]

Neville M, Stutz F, Lee L, Davis LI, and Rosbash M (1997). The importin-beta family member Crm1p bridges the interaction between Rev and the nuclear pore complex during nuclear export. Curr. Biol 7, 767–775. [PubMed: 9368759]

Noordstra I, and Akhmanova A (2017). Linking cortical microtubule attachment and exocytosis. F1000Res 6, 469. [PubMed: 28491287]

Noritake J, Watanabe T, Sato K, Wang S, and Kaibuchi K (2005). IQGAP1: a key regulator of adhesion and migration. J. Cell Sci 118, 2085–2092. [PubMed: 15890984]

Ono A, and Freed EO (1999). Binding of human immunodeficiency virus type 1 Gag to membrane: role of the matrix amino terminus. J. Virol 73, 4136–4144. [PubMed: 10196310]

Ossareh-Nazari B, Bachelerie F, and Dargemont C (1997). Evidence for a role of CRM1 in signal-mediated nuclear protein export. Science 278, 141–144. [PubMed: 9311922]

Pal R, Reitz MS Jr., Tschachler E, Gallo RC, Sarngadharan MG, and Veronese FD (1990). Myristoylation of gag proteins of HIV-1 plays an important role in virus assembly. AIDS Res. Hum. Retroviruses 6, 721–730. [PubMed: 2194551]

Ragheb JA, Yu H, Hofmann T, and Anderson WF (1995). The amphotropic and ecotropic murine leukemia virus envelope TM subunits are equivalent mediators of direct membrane fusion: implications for the role of the ecotropic envelope and receptor in syncytium formation and viral entry. J. Virol 69, 7205–7215. [PubMed: 7474142]

Ren JG, Li Z, Crimmins DL, and Sacks DB (2005). Self-association of IQGAP1: characterization and functional sequelae. J. Biol. Chem 280, 34548–34557. [PubMed: 16105843]

Rosenbluh J, Mercer J, Shrestha Y, Oliver R, Tamayo P, Doench JG, Tirosh I, Piccioni F, Hartenian E, Horn H, et al. (2016). Genetic and proteomic interrogation of lower confidence candidate genes reveals signaling networks in beta-catenin-active cancers. Cell Syst 3, 302–316.e4. [PubMed: 27684187]

Saad JS, Loeliger E, Luncsford P, Liriano M, Tai J, Kim A, Miller J, Joshi A, Freed EO, and Summers MF (2007). Point mutations in the HIV-1 matrix protein turn off the myristyl switch. J. Mol. Biol 366, 574–585. [PubMed: 17188710]

Sabo Y, Walsh D, Barry DS, Tinaztepe S, de Los Santos K, Goff SP, Gundersen GG, and Naghavi MH (2013). HIV-1 induces the formation of stable microtubules to enhance early infection. Cell Host Microbe 14, 535–546. [PubMed: 24237699]

Sayedyahossein S, Li Z, Hedman AC, Morgan CJ, and Sacks DB (2016). IQGAP1 binds to Yes-associated protein (YAP) and modulates its transcriptional activity. J. Biol. Chem 291, 19261–19273. [PubMed: 27440047]

Scarlata S, and Carter C (2003). Role of HIV-1 Gag domains in viral assembly. Biochim. Biophys. Acta 1614, 62–72. [PubMed: 12873766]

Schmidt O, and Teis D (2012). The ESCRT machinery. Curr. Biol 22, R116–R120. [PubMed: 22361144]

Simon S, Schell U, Heuer N, Hager D, Albers MF, Matthias J, Fahrnbauer F, Trauner D, Eichinger L, Hedberg C, and Hilbi H (2015). Inter-kingdom signaling by the legionella quorum sensing molecule LAI-1 modulates cell migration through an IQGAP1-Cdc42-ARHGEF9-dependent pathway. PLoS Pathog 11, e1005307. [PubMed: 26633832]

Smith JM, Hedman AC, and Sacks DB (2015). IQGAPs choreograph cellular signaling from the membrane to the nucleus. Trends Cell Biol 25, 171–184. [PubMed: 25618329]

Strack B, Calistri A, Craig S, Popova E, and Göttlinger HG (2003). AIP1/ALIX is a binding partner for HIV-1 p6 and EIAV p9 functioning in virus budding. Cell 114, 689–699. [PubMed: 14505569]

Sundquist WI, and Kräusslich HG (2012). HIV-1 assembly, budding, and maturation. Cold Spring Harb. Perspect. Med 2, a006924. [PubMed: 22762019]

Superti F, Seganti L, Ruggeri FM, Tinari A, Donelli G, and Orsi N (1987). Entry pathway of vesicular stomatitis virus into different host cells. J. Gen. Virol 68, 387–399. [PubMed: 3029282]

Swanson CM, Puffer BA, Ahmad KM, Doms RW, and Malim MH (2004). Retroviral mRNA nuclear export elements regulate protein function and virion assembly. EMBO J 23, 2632–2640. [PubMed: 15201866]

Tian Y, Tian X, Gawlak G, O'Donnell JJ 3rd, Sacks DB, and Birukova AA (2014). IQGAP1 regulates endothelial barrier function via EB1-cortactin cross talk. Mol. Cell. Biol 34, 3546–3558. [PubMed: 25022754]

VerPlank L, Bouamr F, LaGrassa TJ, Agresta B, Kikonyogo A, Leis J, and Carter CA (2001). Tsg101, a homologue of ubiquitin-conjugating (E2) enzymes, binds the L domain in HIV type 1 Pr55(Gag). Proc. Natl. Acad. Sci. USA 98, 7724–7729. [PubMed: 11427703]

Votteler J, and Sundquist WI (2013). Virus budding and the ESCRT pathway. Cell Host Microbe 14, 232–241. [PubMed: 24034610]

Wagner R, Graf M, Bieler K, Wolf H, Grunwald T, Foley P, and Uberla K (2000). Rev-independent expression of synthetic gag-pol genes of human immunodeficiency virus type 1 and simian immunodeficiency virus: implications for the safety of lentiviral vectors. Hum. Gene Ther 11, 2403–2413. [PubMed: 11096444]

Watanabe T, Wang S, and Kaibuchi K (2015). IQGAPs as key regulators of actin-cytoskeleton dynamics. Cell Struct. Funct 40, 69–77. [PubMed: 26051604]

Whisenant TC, Peralta ER, Aarreberg LD, Gao NJ, Head SR, Ordoukhanian P, Williamson JR, and Salomon DR (2015). The activation-induced assembly of an RNA/protein interactome centered on the splicing factor U2AF2 regulates gene expression in human CD4 T cells. PLoS ONE 10, e0144409. [PubMed: 26641092]

White CD, Erdemir HH, and Sacks DB (2012). IQGAP1 and its binding proteins control diverse biological functions. Cell. Signal 24, 826–834. [PubMed: 22182509]

Yoshimoto T, Yoshimoto E, and Meruelo D (1993). Identification of amino acid residues critical for infection with ecotropic murine leukemia retrovirus. J. Virol 67, 1310–1314. [PubMed: 8382297]

Yueh A, and Goff SP (2003). Phosphorylated serine residues and an arginine-rich domain of the moloney murine leukemia virus p12 protein are required for early events of viral infection. J. Virol 77, 1820–1829. [PubMed: 12525616]

Zhang Y, and Barklis E (1997). Effects of nucleocapsid mutations on human immunodeficiency virus assembly and RNA encapsidation. J. Virol 71, 6765–6776. [PubMed: 9261401]

Zhou W, and Resh MD (1996). Differential membrane binding of the human immunodeficiency virus type 1 matrix protein. J. Virol 70, 8540–8548. [PubMed: 8970978]

Highlights

- Depletion of IQGAP1 increases HIV-1 viral particle release
- Overexpression of IQGAP1 reduces HIV-1 viral particle release
- IQGAP1 interacts with the NC and p6 domains of the HIV-1 Gag protein
- IQGAP1 negatively regulates HIV-1 Gag accumulation at the plasma membrane

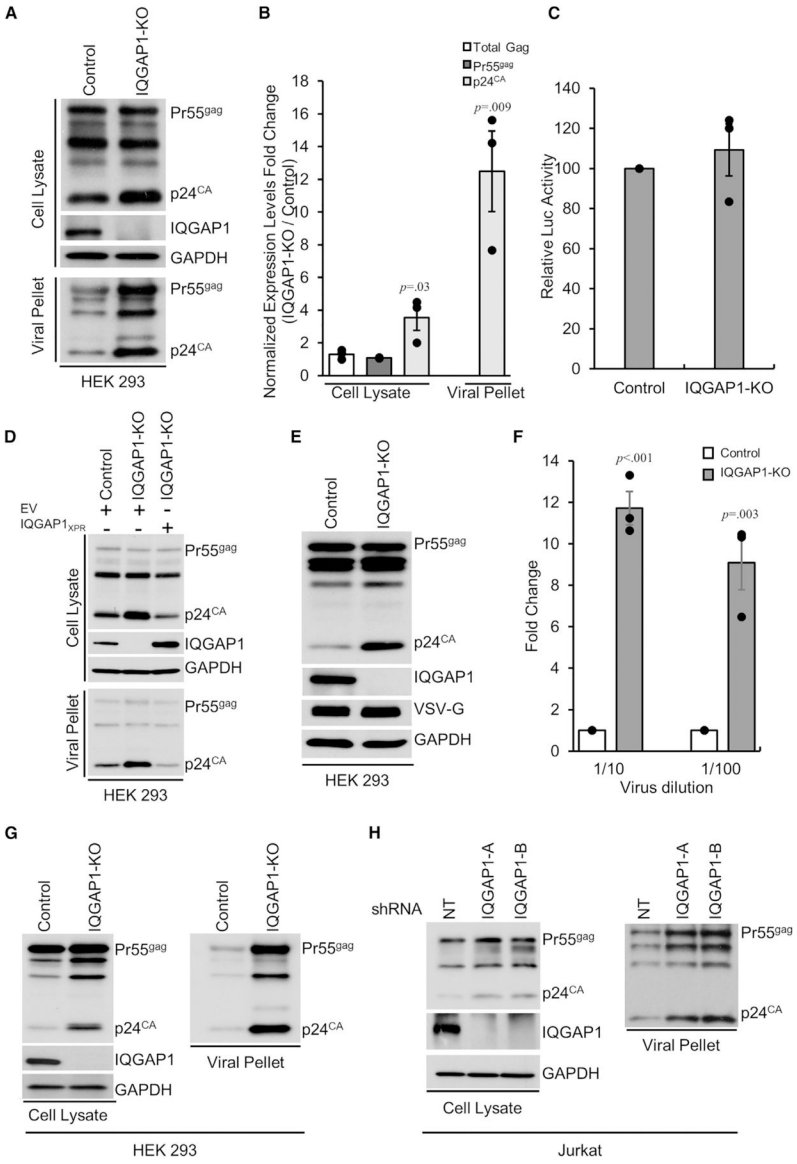

Figure 1. Depletion of IQGAP1 Increases Production of Infectious HIV-1 Virions

(A) KO of IQGAP1 in HEK293 cells increases release of HIV-1 virions. IQGAP1 KO and control HEK293 cells were transfected with HIV-1 viral genome (pNL4–3.Luc.R-E-; 1 μg). After 48 h the culture supernatants were collected, and the cells were harvested and lysed. Virions in the supernatants were isolated by pelleting through 25% sucrose cushions. Gag protein and its cleavage products in the cells (cell lysate) and in released virions (viral pellet) were detected by HIV-1-specific antibody. Shown are representative western blots from three independent experiments (n = 3).

(B) Densitometric analysis of data in (A). Shown are fold changes in protein expression levels for total Gag (Pr55^{gag} and all its cleavage products), Pr55^{gag}, and p24^{CA} relative to control transfected cells, all normalized to GAPDH for each experiment. The data are mean ± SEM from three independent experiments (n = 3). p values are shown when increase of p24^{CA} from KO cells relative to control cells is significant.

(C) KO of IQGAP1 in HEK293 cells does not affect expression of viral genomes. Cell lysates from (A) were assayed to measure the luciferase reporter expressed from the Nef ORF in the transfected viral genomes, with the levels in the control transfected cells set at 100. The data are mean ± SEM from three independent experiments (n = 3).

(D) Re-expression of WT IQGAP1 in IQGAP1 KO cells reduces HIV-1 viral release to normal levels of control cells. IQGAP1-KO cells were co-transfected with pNL4–3.Luc.R-E-viral DNA genome (1 μg) and either an empty vector (EV) or a CRISPR-resistant IQGAP1-expressing DNA ($IQGAP1_{XPR}$) Control cells were co-transfected with HIV-1 viral genome (pNL4–3.Luc.R-E-; 1 μg) and an empty vector (EV). All transfection were performed at a molar ratio of 3:1 (EV or $IQGAP1_{XPR}$ to pNL4–3.Luc.R-E-). After 48 h culture supernatants and cells were processed as in (A). Shown are representative western blots from three independent experiments (n = 3).

(E) Expression of HIV-1 proteins with VSV-G in IQGAP1-depleted cells. IQGAP1 KO or control HEK293 cells were transfected with HIV-1 viral genome (pNL4–3.Luc.R-E-; 1 μg) and pVSVG (0.5 μg). At 48 h after transfection, the cells were harvested and lysed. Intracellular Gag protein and its cleavage products as well as the VSV-G env protein were detected with specific antibodies. Shown is a representative western blot out of three independent experiments (n = 3).

(F) KO of IQGAP1 enhances the production of infectious HIV-1 virus. Two serial dilutions (1/10 and 1/100) of culture supernatants harvested from producer cells in (E) were used to infect HEK293A cells, and luciferase activities were measured 48 h after infection. In each infecting dilution, the luciferase activity from cells infected with virus packaged from control cells was set as 1. The data are mean ± SEM and p values are for virus yield from KO cells relative to control cells from three independent experiments (n = 3).

(G) KO of IQGAP1 increases release of HIV-1 virions from infected cells. IQGAP1 KO and control HEK293 cells were infected with HIV-1-VSV for 48 h. Cell lysates (cell lysate) and culture supernatants (viral pellet) were assessed by western blots as in (A). Shown are representative western blots from three independent experiments (n = 3).

(H) KD of IQGAP1 in human T cell lymphoblast-like cell line increases release of HIV-1 virions from infected cells. Stable KO Jurkat cells expressing specific IQGAP1 shRNAs (IQGAP-A and IQGAP1-B) or expressing control non-targeting (NT) shRNA were infected and processed as in (G). Shown are representative western blots from three independent experiments (n = 3).

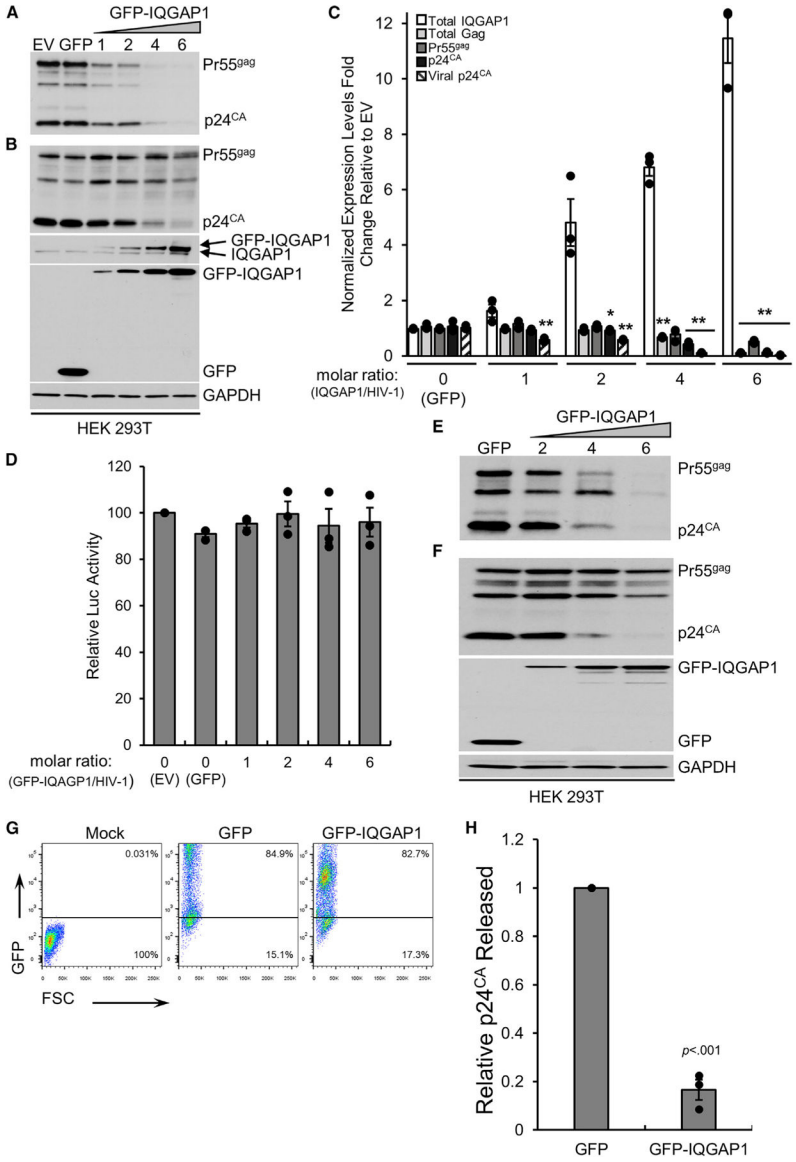

Figure 2. IQGAP1 Overexpression Reduces Viral Particle Release

(A and B) GFP-IQGAP1 overexpression reduces viral release in a dose-dependent manner. HEK293T cells were co-transfected with HIV-1 viral genome (pNL4–3.Luc.R-E-; 0.5 μg) together with an empty vector (EV) or GFP or an increasing amounts of DNA expressing GFP-IQGAP1, ranging from a molar ratio (GFP-IQGAP1/pNL4–3.Luc.R-E-) of 1–6, and an empty vector to ensure equal total amount of transfected DNA. After 48 h the cells were lysed, and virions in the supernatants were isolated. Gag and $p24^{CA}$ levels in pelleted virions (A) and cellular Gag protein and its cleavage products, endogenous IQGAP1, GFP, and GFP-IQGAP1 expression levels (B) were assessed using western blot with specific anti-HIV-1 Gag, anti-IQGAP1, or anti-GFP antibodies. Shown are representative western blots from three independent experiments (n = 3).

(C) Densitometric analysis of data presented in (A) and (B). Shown are fold changes in protein expression levels of total IQGAP1 (endogenous and exogenous GFP-IQGAP1 levels

as measured using the anti-IQGAP1 antibody), total Gag ($Pr55^{gag}$ and all its cleavage products), $Pr55^{gag}$, and cellular and viral $p24^{CA}$, relative to EV transfected cells, all normalized to GAPDH for each experiment. The data are mean ± SEM, and p values are for indicated viral protein with IQGAP1 overexpression relative to EV control, from three independent experiments (n = 3). *p = 0.022 and **p < 0.001.

(D) IQGAP1 overexpression does not affect expression of reporter genes on viral genome. Cell lysates from (A) were subjected to luciferase assays. The luciferase activity measured in the empty vector (EV) transfected control cells was set as 100. The data are mean ± SEM from three independent experiments (n = 3).

(E and F) IQGAP1 overexpression reduces VLPs release from a Rev-independent HIV-1 Gag-Pol expression construct. HEK293T cells were co-transfected with a DNA encoding Rev-independent Gag-Pol (0.5 μg) together with DNA encoding GFP or increasing levels of DNA encoding GFP-IQGAP1 at a molar ratio (GFP-IQGAP1/Rev-independent Gag-Pol) ranging from 2 to 6 and processed as in (A) and (B). Pelleted virion proteins (E) and intracellular proteins (F). Shown are representative western blots from three independent experiments (n = 3).

(G and H) IQGAP1 overexpression reduces HIV-1 viral release from infected cells. HEK293T cells were transfected with GFP or GFP-IQGAP1(2.5 μg) for 24 h, followed by infection with HIV-1-VSV for an additional 48 h.

(G) Flow cytometry measurement of GFP expression in infected cells.

(H) Relative amount of $p24^{CA}$ released to culture supernatant as measured by HIV-1 p24 ELISA. $p24^{CA}$ amount measured in the GFP-transfected cells was set as 1. The data are mean ± SEM, and p value is for released $p24^{CA}$ with IQGAP1 overexpression relative to control, from three independent experiments (n = 3).

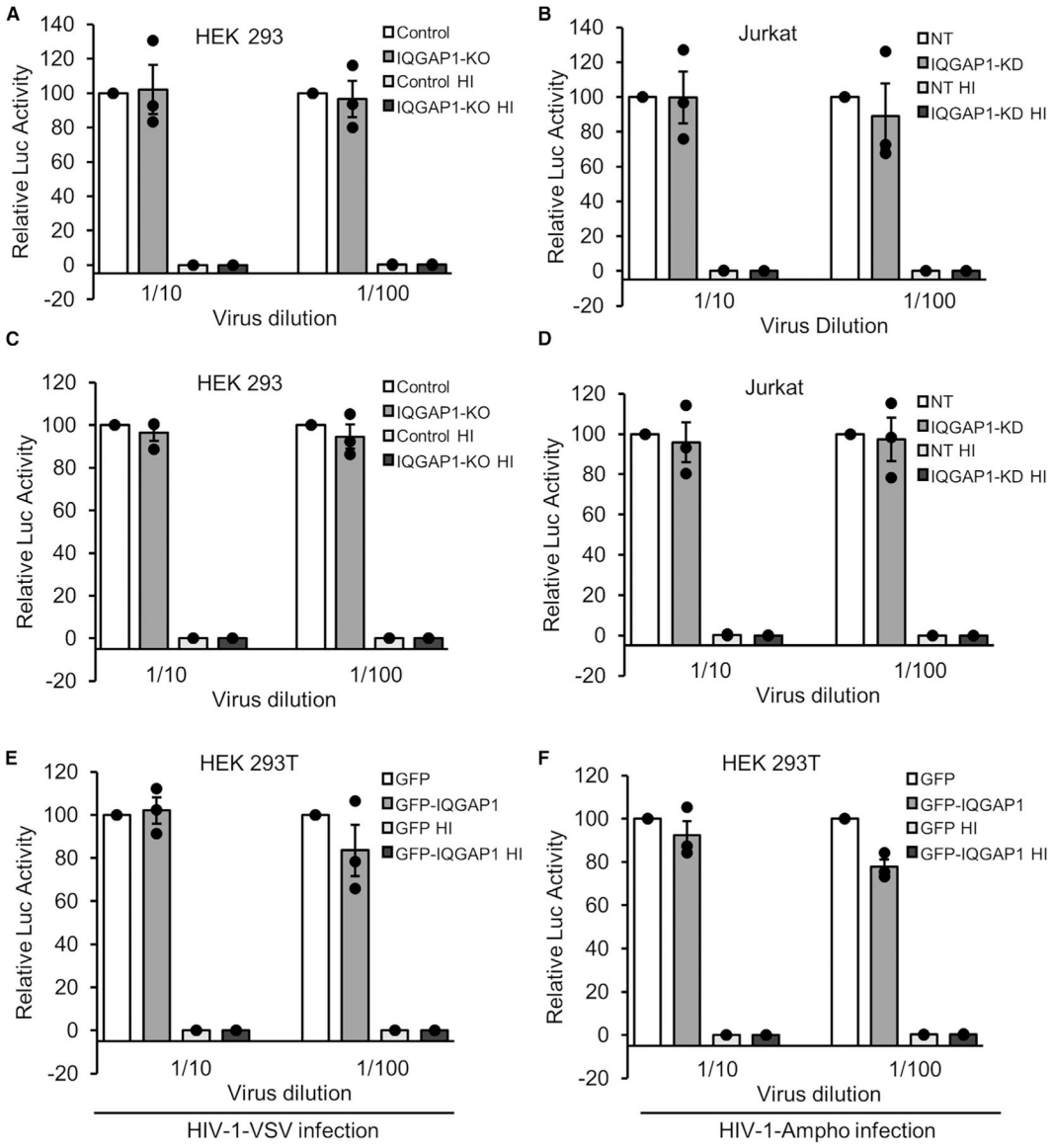

Figure 3. Depletion or Overexpression of IQGAP1 Does Not Affect the Viral Early Stages of the Life Cycle

(A and B) Depletion of IQGAP1 does not affect the viral early stages of cells infected with HIV-1-VSV. IQGAP1 KO and control HEK293 cells (A) or stable IQGAP1 KD and non-targeting shRNA control (NT) Jurkat cells (B) were infected with two serial dilutions (1/10 and 1/100) of HIV-1-VSV, or heat-inactivated HIV-1-VSV (HI), which served as a negative control for the infection, for 48 h. Cell lysates were assayed to measure the luciferase levels expressed from the integrated provirus. Luciferase activity measured in control or NT-infected cells was set as 100. The data are mean ± SEM from three independent experiments (n = 3).

(C and D) Depletion of IQGAP1 does not affect the viral early stages in cells infected with HIV-1-Ampho. IQGAP1 KO and control HEK293 cells (C) or stable IQGAP1 KD and non-targeting shRNA control (NT) Jurkat cells (D) were infected with two serial dilutions (1/10 and 1/100) of HIV-1-Ampho or heat-inactivated HIV-1-Ampho (HI), which served as a

negative control for the infection, for 48 h and processed as in (A). Luciferase activity measured in control or NT-infected cells was set as 100. The data are mean ± SEM from three independent experiments (n = 3).

(E and F) Overexpression of IQGAP1 does not affect the viral early stages of infected cells. HEK293T cells were transfected with either GFP or GFP-IQGAP1 (2.5 μg) for 24 h. Cells were then infected for additional 48 h with (E) HIV-1-VSV or heat-inactivated HIV-1-VSV (HI) or (F) HIV-1-Ampho viruses or heat-inactivated HIV-1-Ampho (HI) and processed as in (A). HI viruses served as a negative control for the infection. The luciferase activity measured in GFP infected cells was set as 100. The data are mean ± SEM from three independent experiments (n = 3).

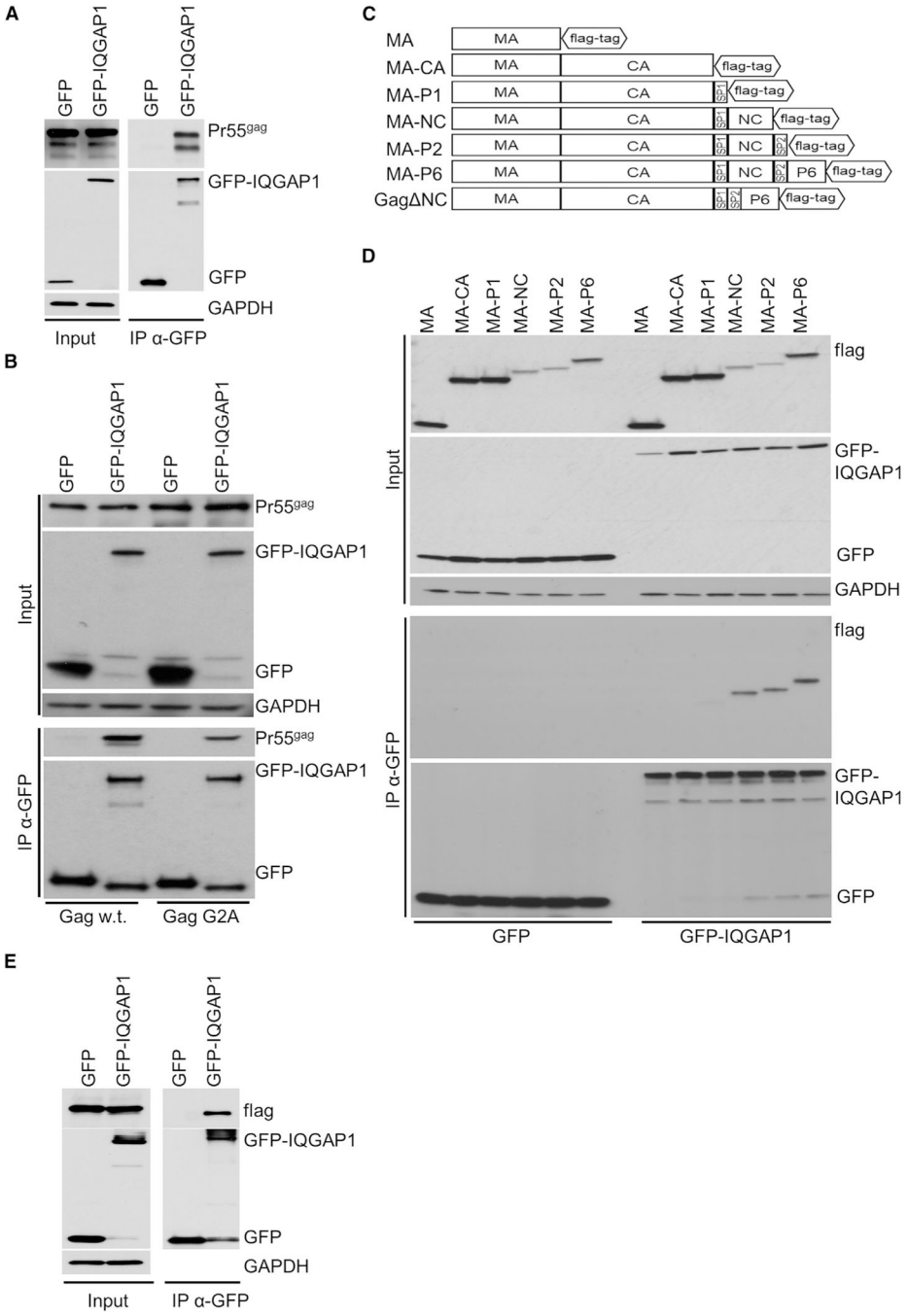

Figure 4. IQGAP1 Interacts with the Nucleocapsid and p6 Domains of HIV-1 Gag

(A) IQGAP1 interacts with the HIV-1 Gag protein. HEK293T cells were co-transfected with HIV-1 viral genome (pNL4–3.Luc.R-E-; 1 μg) together with DNAs expressing GFP or GFP-IQGAP1 at a molar ratio of 3 (GFP or GFP-IQGAP1 to pNL4–3.Luc.R-E-). Cell lysates were subjected to immunoprecipitation using anti-GFP antibody. GFP, GFP-IQGAP1, and Gag were detected using western blot. Shown are representative western blots from three independent experiments (n = 3).

(B) IQGAP1 interacts with unmyristylated HIV-1 Gag protein. HEK293T cells were co-transfected with HIV-1 viral genome (Gag WT; 1 μg) or with an HIV-1 genome encoding a Gag mutant that cannot be myristylated (Gag G2A; 1 μg) together with DNAs encoding GFP or GFP-IQGAP1 at a molar ratio of 3 (GFP or GFP-IQGAP1 to Gag WT or Gag G2A) and processed as in (A). Shown are representative western blots from three independent experiments (n = 3).

(C) Schematic presentation of the Rev-independent flag-tagged Gag domains proteins used for this experiment.

(D) The nucleocapsid domain of Gag interacts with IQGAP1. HEK293T cells were co-transfected with DNAs encoding GFP or GFP-IQGAP1 together with 1 μg of the indicated Gag constructs from (C) at a molar ratio of 3 (GFP or GFP-IQGAP1 to HIV-1 Gag constructs) and processed as in (A). Shown are representative western blots from three independent experiments (n = 3).

(E) The p6 domain of Gag interacts with IQGAP1. HEK293T cells were co-transfected with the GagDNC construct (C) (1 μg) together with DNAs encoding GFP or GFP-IQGAP1 at a molar ratio of 3 (GFP or GFP-IQGAP1 to GagΔDNC) and processed as in (A). Shown are representative western blots from three independent experiments (n = 3).

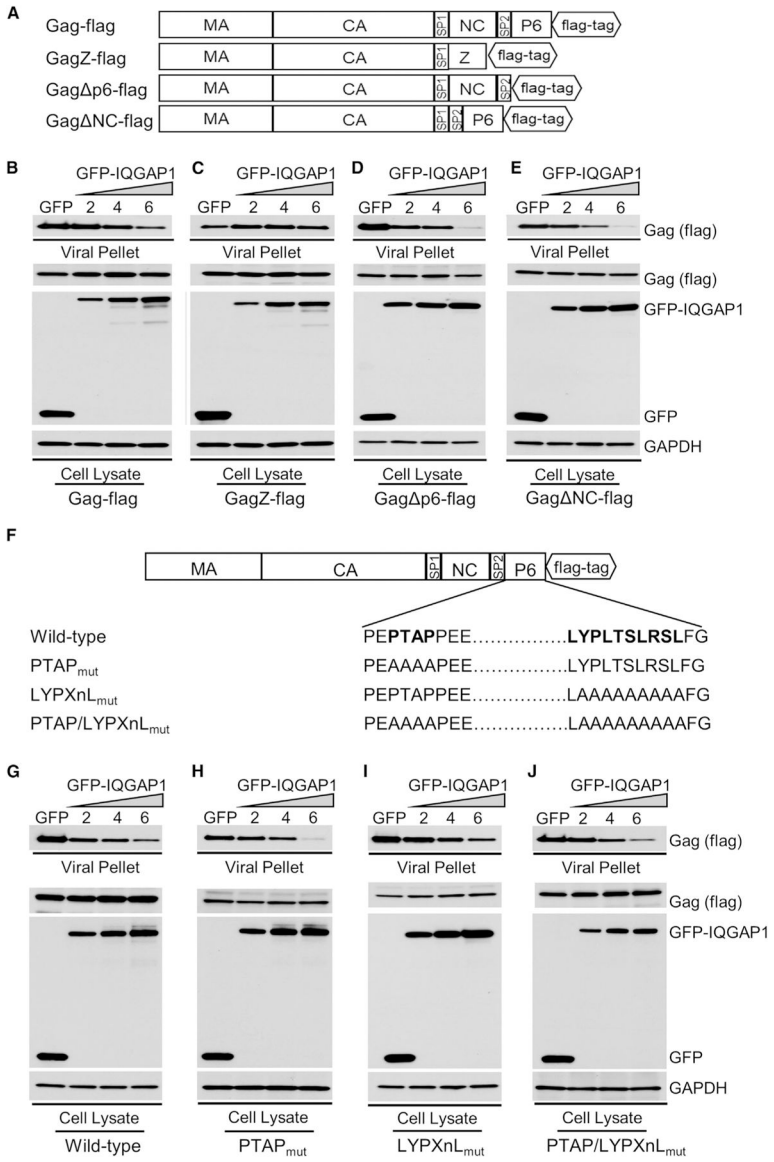

Figure 5. The C Terminus Region of HIV-1 Gag Is Required for IQGAP1 Regulation of Viral Release Independently of Gag L Domains

(A) Schematic presentation of Rev-independent flag-tagged Gag domains proteins used for this experiment.

(B and C) Replacement of the C terminus region of Gag with the GCN4 leucine zipper abolishes IQGAP1 regulation of HIV-1 VLP release. HEK293T cells were co-transfected with Rev-independent Gag-flag (B) or GagZ-flag (C) constructs (0.5 μg) with increasing amounts of DNA encoding GFP-IQGAP1 or GFP at a molar ratio (GFP-IQGAP1 to HIV-1 Gag DNAs) ranging from 2 to 6 and an empty vector to ensure equal total amount of transfected DNAs. After 48 h, cells were lysed and virions in the culture supernatants were purified. CA levels in pelleted virions and intracellular GFP-IQGAP1 and Gag levels were assessed using western blot with specific anti-GFP or anti-flag antibodies. Shown are representative western blots from three independent experiments (n = 3).

(D and E) Either the p6 or the nucleocapsid domains in Gag are sufficient for IQGAP1 negative regulation of HIV-1 VLP release. HEK293T cells were co-transfected with Rev-independent GagΔp6-flag (D) or GagDNC-flag (E) DNAs (0.5 μg) together with increasing amounts of DNAs encoding GFP or GFP-IQGAP1 at a molar ratio (GFP-IQGAP1 to HIV-1 Gag DNAs) ranging from 2 to 6 and an empty vector to ensure equal total amount of transfected DNA and processed as in (B). Shown are representative western blots from three independent experiments (n = 3).

(F) Schematic presentation of Rev-independent flag-tagged Gag mutant proteins used for this research.

(G–J) IQGAP1 overexpression reduces HIV-1 Gag VLPs lacking the ability to recruit the cellular ESCRT machinery. HEK293T cells were co-transfected with DNA constructs from (F) (0.5 μg) together with increasing amounts of DNAs encoding GFP or GFP-IQGAP1 at a molar ratio (GFP-IQGAP1 to HIV-1 Gag DNAs) ranging from 2 to 6 and an empty vector to ensure equal total amount of transfected DNAs. After 48 h, cells were lysed and virions in the supernatants were isolated. CA levels in pelleted virions and cellular GFP-IQGAP1 and Gag expression levels were assessed using western blot with specific anti-GFP or anti-flag antibodies. Cells were transfected with (G) wild-type, (H) PTAPmut, (I) LYPXnLmut, (J) and PTAP/LYPXnLmut Gag expression constructs. Shown are representative western blots from three independent experiments (n = 3).

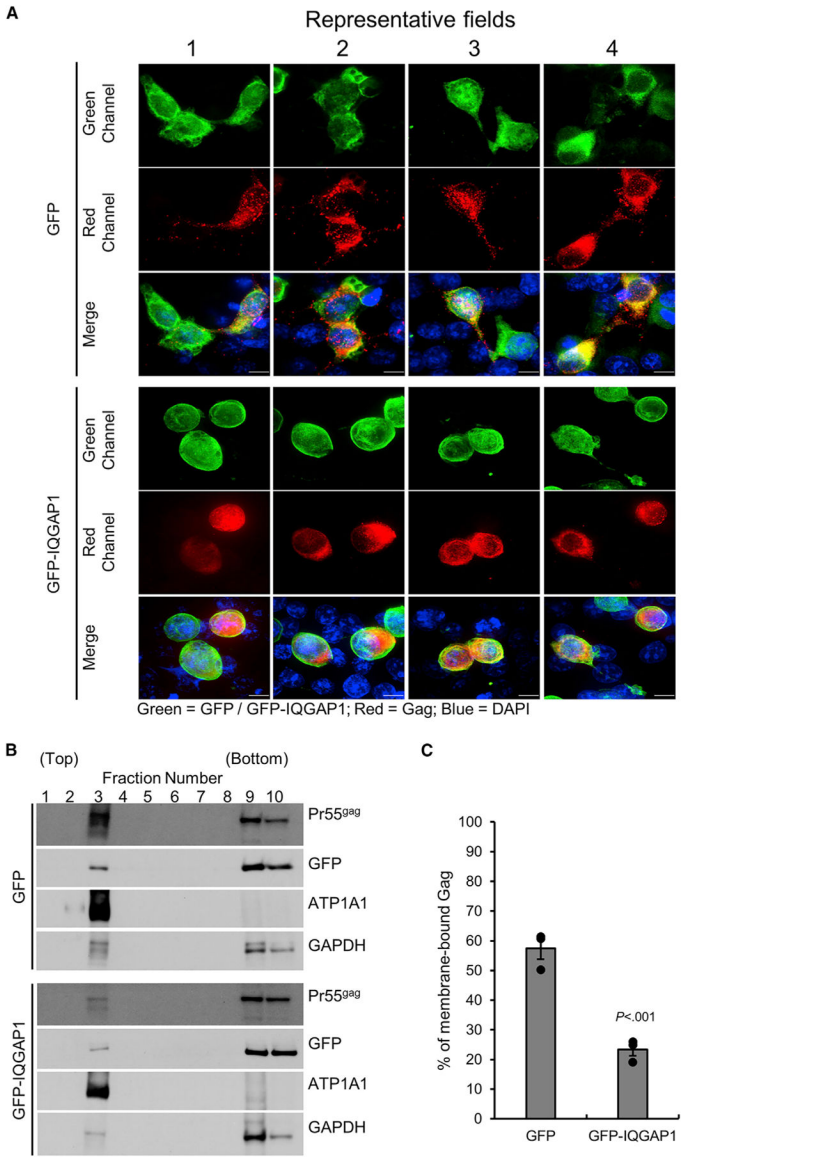

Figure 6. IQGAP1 Overexpression Restricts HIV-1 Gag Targeting to the Plasma Membrane

(A) Overexpression of IQGAP1 reduces the steady-state levels of membrane-bound Gag. HEK293T cells were co-transfected with HIV-1 viral genome (pNL4–3.Luc.R-E-; 1 μg) together with DNA encoding GFP or GFP-IQGAP1 at a molar ratio of 4 (GFP or GFP-IQGAP1 to pNL4–3.Luc.R-E-) After 48 h, the cells were fixed and stained for HIV-1 Gag (red) and GFP/GFP-IQGAP1 (green) using specific antibodies and for the cell nuclei using DAPI (blue). Random fields of view were imaged to acquire a minimum of 100 GFP/GFP-IQGAP1-expressing cells. Shown are four representative fields of view from a single experiment out of three independent experiments (n = 3). Scale bar, 10 μm.

(B) 293T cells were transfected as in (A), and 48 h after transfection, membrane floatation assay was used to determine the distribution of Gag in the cytosol and membrane fractions as detected using western blot. ATP1A1 is used as a membrane fraction marker, and

GAPDH is used as a cytosol fraction marker. Shown are representative western blots from three independent experiments (n = 3).

(C) Densitometric analysis of the data in (B). Percentage of membrane-bound Gag was calculated on the basis of densitometry measurements of total (cytoplasmic and membrane) and membrane-bound Gag. The data are mean ± SEM from three independent experiments (n = 30). p value is for membrane-bound Gag with GFP-IQGAP1 overexpression relative to GFP control.

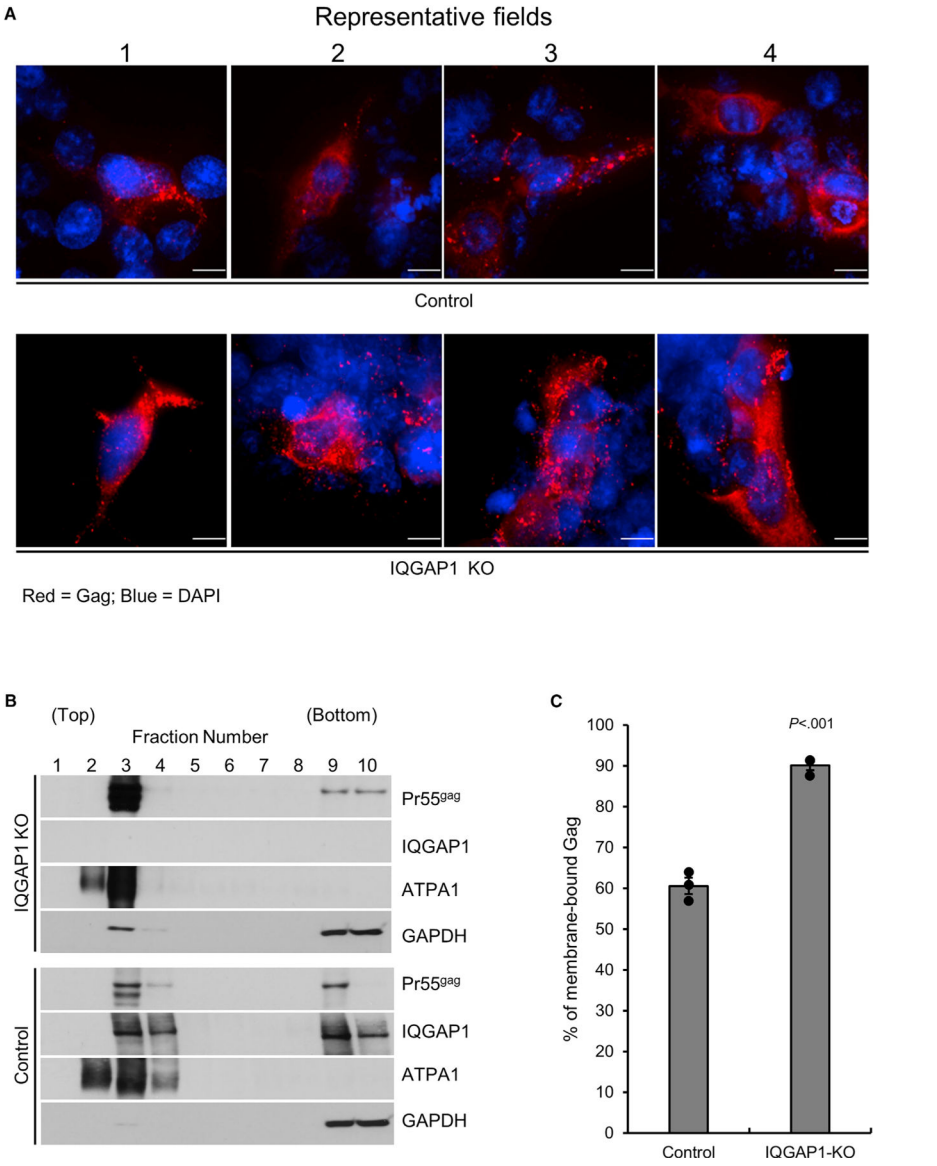

Figure 7. IQGAP1 Depletion Enhances HIV-1 Gag Targeting to The Plasma Membrane

(A) Depletion of IQGAP1 enhances Gag association to the plasma membrane. Control or IQGAP1 KO HEK293 cells were transfected with HIV-1 viral genome (pNL4–3.Luc.R-E-; 1 μg). After 48 h, the cells were fixed and stained for HIV-1 Gag using HIV-1-specific antibody (red) and for cell nuclei using DAPI (blue). Random fields of view were imaged to acquire a minimum of 100 Gag-expressing cells. Shown are four representative fields of view from a single experiment out of three independent experiments (n = 3). Scale bar, 10 μm.

(B) IQGAP1 KO or control cells were transfected as in (A), and membrane floatation assay was performed as in Figure 6B. Shown are representative western blots from three independent experiments (n = 3).

(C) Densitometric analysis of the data in (B) was calculated as described in Figure 6C. The data are mean ± SEM from three independent experiments (n = 3). p value is for membrane-bound Gag in IQGAP1-KO cells relative to control.

KEY RESOURCES TABLE

REAGENT or RESOURCE	SOURCE	IDENTIFIER
Antibodies		
Anti-HIV1 p24 antibody [39/5.4A]	Abcam	Cat# ab9071;RRID:AB_306981
Recombinant Anti-IQGAP1 antibody [EPR5220]	Abcam	Cat# ab133490; RRID:AB_11157518
Anti-GFP antibody [EPR14104]	Abcam	Cat# ab183734; RRID:AB_2732027
ANTI-FLAG® antibody produced in rabbit	Sigma	Cat# F7425; RRID:AB_439687
Anti-GFP antibody	Abcam	Cat# ab13970; RRID:AB_300798
Anti-GAPDH Mouse mAb (6C5)	Millipore Sigma	Cat# CB1001; RRID:AB_2107426
Anti-VSV-G antibody produced in rabbit	Sigma	Cat# V4888; RRID:AB_261872
Anti-Sodium Potassium ATPase antibody [EP1845Y] -Plasma Membrane Loading Control	Abcam	Cat# ab76020; RRID:AB_1310695
Anti-Tubulin antibody [YL1/2]	Abcam	Cat# ab6160; RRID:AB_305328
Purified anti-HA.11 Epitope Tag Antibody	Biolegend	Cat# 901501
goat anti-MuLV CA polyclonal antibody	National Cancer Institute	product no. 81S-263
Rabbit IgG HRP Linked Whole Ab	Millipore Sigma	Cat# NA934; RRID:AB_772206
Mouse IgG HRP Linked F(ab′)2 Fragment	Millipore Sigma	Cat# NA9310; RRID:AB_772193
Donkey Anti-Goat IgG H&L (HRP) (ab97110)	Abcam	Cat# ab97110; RRID:AB_10679463
Goat anti-Chicken IgY (H+L) Secondary Antibody, Alexa Fluor 488	ThermoFisher	Cat# A-11039; RRID:AB_142924
IgG (H+L) Cross-Adsorbed Goat anti-Rat, Alexa Fluor® 647	ThermoFisher	Cat# A-21247; RRID:AB_141778
Goat anti-Mouse IgG (H+L) Highly Cross-Adsorbed Secondary Antibody, Alexa Fluor 555	ThermoFisher	Cat# A-21424; RRID:AB_141780
Chemicals, Peptides, and Recombinant Proteins		
Trypan Blue Solution	ThermoFisher	Cat# 15250061
lipofectamine 2000	ThermoFisher	Cat# 11668019
Lipofectamine RNAiMAX	ThermoFisher	Cat# 13778150
polybrene	Millipore Sigma	Cat# TR-1003-G
PVDF membrane	Millipore Sigma	Cat# IPFL00010
CelLytic M Cell Lysis Reagent	Sigma	Cat# C2978
4x Laemmli Sample Buffer	BIO-RAD	Cat# 161–0747
RQ1 RNase-Free DNase	Promega	Cat# M6101
Ambion RNase A, affinity purified	ThermoFisher	Cat# AM2271
DAPI	Sigma	D9564–10MG
FluorSave Reagent	Millipore Sigma	Cat# 345789–20ML
Puromycin dihydrochloride	Sigma	P9620–10ML
FastStart Universal SYBR Green Master (Rox)	Millipore Sigma	Cat# 4913850001
Critical Commercial Assays		
HIV-1 p24 SimpleStep ELISA Kit	Abcam	Cat# ab218268
Luciferase Assay System	Promega	Cat# E4550
DNeasy Blood and Tissue Kit	Qiagne	Cat# 69506
QIAquick Gel Extraction Kit	QIAGEN	Cat# 28706

REAGENT or RESOURCE	SOURCE	IDENTIFIER
Experimental Models: Cell Lines		
NHDF	Lonza	Cat# CC-2509
HEK293T	ATCC	Cat# CRL-11268
Jurkat	ATCC	Cat# TIB-152
HEK293 (IQGAP1 KO)	Dr. David B. Sacks Lab (Sayedyahossein et al., 2016)	N/A
HEK293 (Control)	Dr. David B. Sacks Lab (Sayedyahossein et al., 2016)	N/A
Oligonucleotides		
DNA fragments (gBlocks) for cloning, see Table S1	This paper	N/A
Primers, see Table S2	This paper	N/A
Non-targeting control siRNAs	Dharmacon	Cat# D-001810–10
IQGAP1 siRNAs	Dharmacon	Cat# L-004694–00-0005
Scrambled shRNA	Dharmacon	Cat# RHS6848
IQGAP1 shRNAs	Dharmacon	Cat# TRCN000004748, TRCN0000047485
Recombinant DNA		
Plasmid: pEGFP-C1	Clontech	Cat# 6085–1
Plasmid: pCDNA4/TO	ThermoFisher	Cat# V102020
Plasmid: pEGFP-IQGAP1	Addgene (Ren et al., 2005)	plasmid # 30112
Plasmid: pNL4–3.Luc.E-.R-	NIH AIDS Reagent Repository (Connor et al., 1995)	Cat# 3418
Plasmid: pHA-mCAT	Dr. Walther Mothes; Yale University School of Medicine	N/A
Plasmid: pNCS	S.P.Goff (Yueh and Goff, 2003)	N/A
Plasmid: pCDNA-4/TO-IQGAP1	This paper	N/A
Plasmid: pEGFP-IQGAP1-XPR-res	This paper	N/A
Plasmid: pCDNA4-IQGAP1-XPR-res	This paper	N/A
Plasmid: Gag G2A	This paper	N/A
Plasmid: pCDNA4-MA-flag	This paper	N/A
Plasmid: pCDNA4-MA-CA-flag	This paper	N/A
Plasmid: pCDNA4-MA-P1-flag	This paper	N/A
Plasmid: pCDNA4-MA-NC-flag	This paper	N/A
Plasmid: pCDNA4-MA-P2-flag	This paper	N/A
Plasmid: pCDNA4-MA-P6-flag	This paper	N/A
Plasmid: pCDNA4-GagΔNC-flag	This paper	N/A
Plasmid: pCDNA4-Gag-flag	This paper	N/A
Plasmid: pCDNA4-GagZ-flag	This paper	N/A
Plasmid: pCDNA4-GagΔP6-flag	This paper	N/A
Plasmid: pCDNA4-Gag-PTAP$_{mut}$-flag	This paper	N/A
Plasmid: pCDNA4-Gag-LYPXnL$_{mut}$-flag	This paper	N/A
Plasmid: pCDNA4-Gag-PTAP/LYPXnL$_{mut}$-flag	This paper	N/A
Software and Algorithms		
ImageJ	Software	ImageJ; RRID: SCR_003070 https://imagej.nih.gov/ij/download.html

REAGENT or RESOURCE	SOURCE	IDENTIFIER
FlowJo	BD Biosciences	Version 10 https://www.flowjo.com/solutions/flowjo/downloads
SlideBook	Intelligent Imaging Innovations (3i)	SlideBook; RRID:SCR_014300 https://www.intelligent-imaging.com/slidebook
BD FACSDiva Version 8.0	BD Biosciences	RRID: SCR_001456 https://www.bdbiosciences.com/en-us